Receptor tyrosine and serine-threonine kinases

Sudarshan Rajagopal

Departments of Medicine and Biochemistry

sudarshan.rajagopal@duke.edu

Receptor Tyrosine Kinases

Timeline 1 | **Breakthrough discoveries on RTK signal transduction and RTK-based cancer therapy**

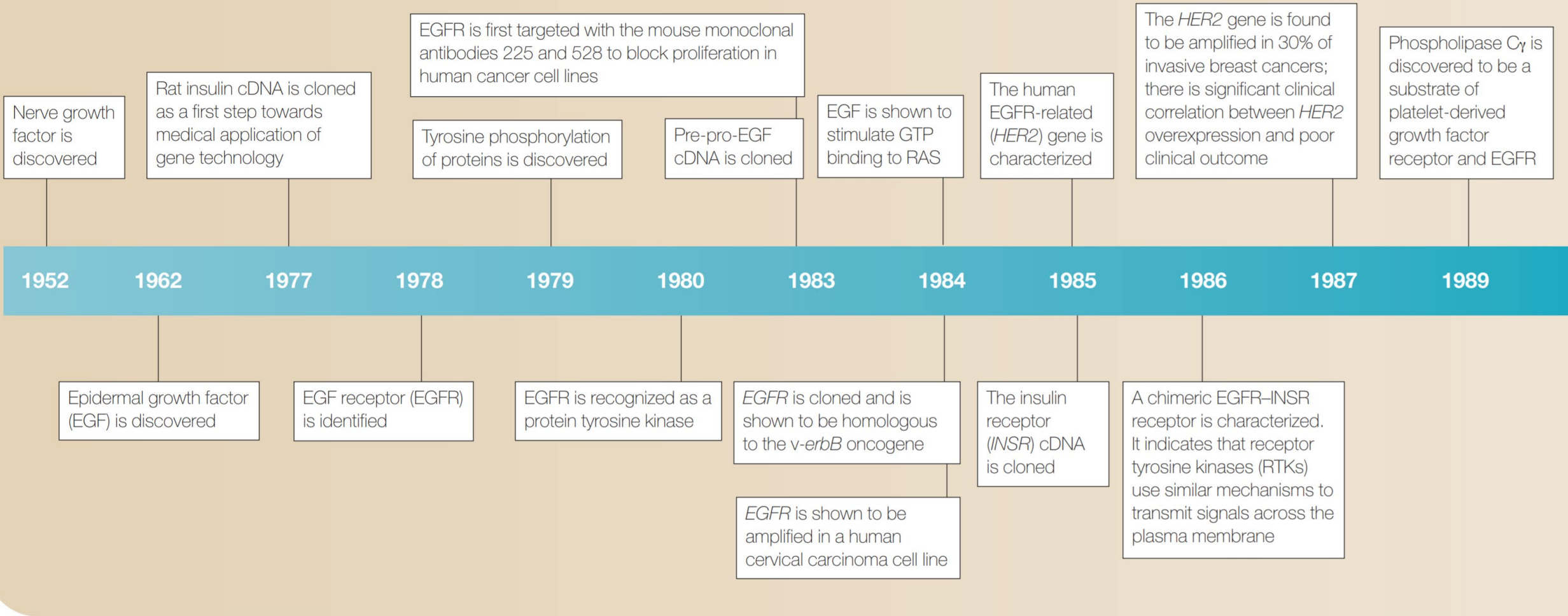

Levi-Montalcini: NGF

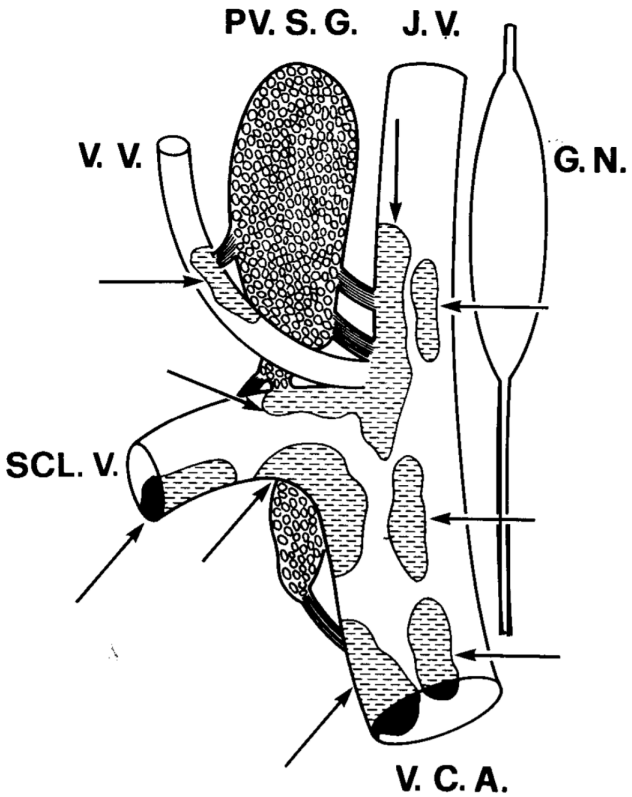

Fig 1. Sixteen-day chick embryo with intra-embryonic tumor (sarcoma 180). Ingrowth of sympathetic nerve fibers into the Jugular, Vertebral, Subclavian Anterior Caval Veins. GN, Ganglium Nodosum; JV, Jugular Vein; Pv.SG, Paravertebral Sympathetic Ganglion; SCL.V, Subclavian Vein; VCA, Anterior Caval Vein; VV, Vertebral Vein. Arrows point to nerve agglomerations. (from Ref. 12)

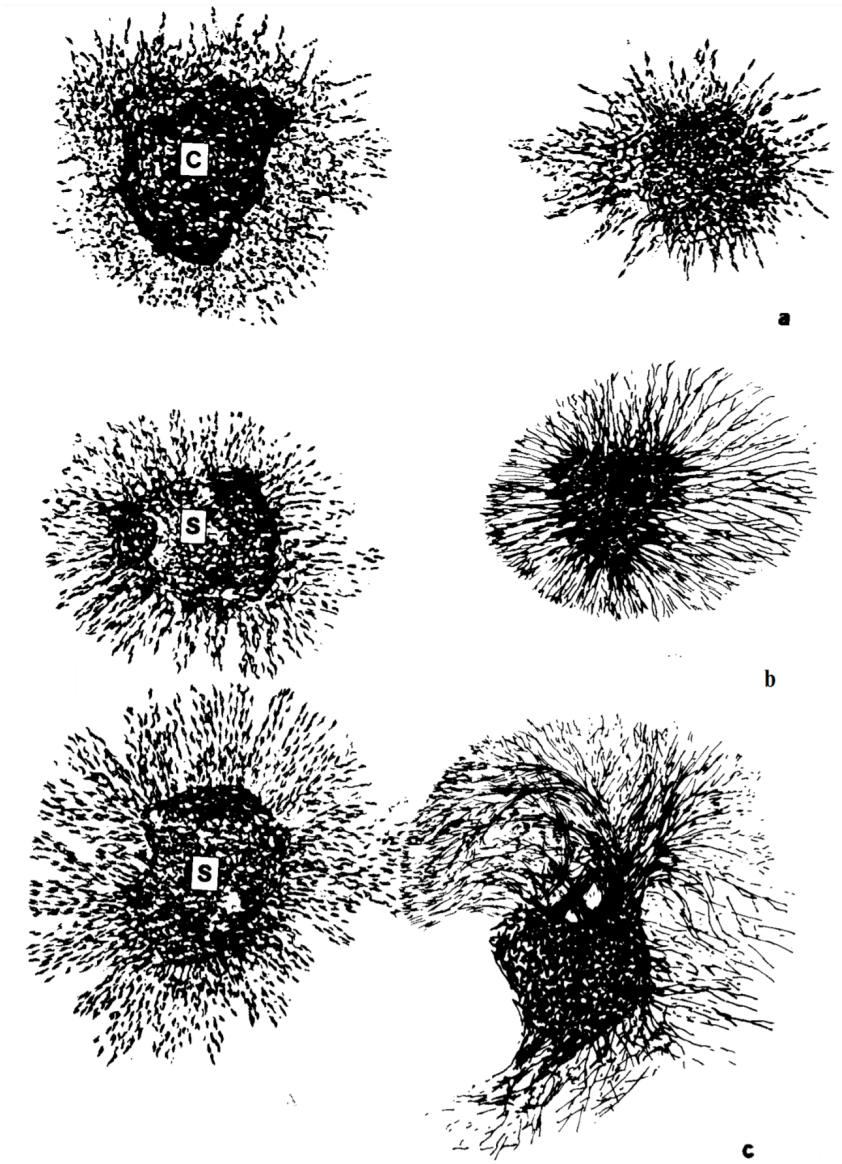

Cohen: EGF

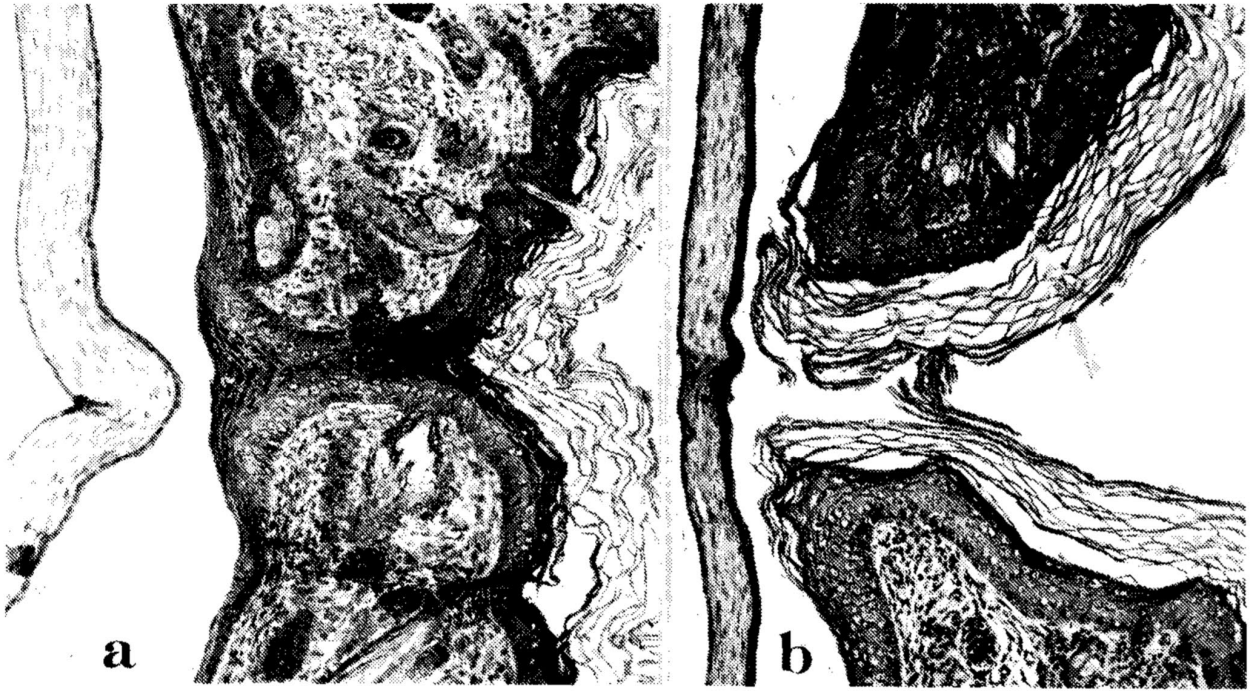

Figure la and b. Cross sections of the eyelid area from control, la, and experimental, lb, 8-day-old rats. The experimental animal had received daily injections (1 µg per 1 gm body weight) of the active protein. × 100. (reprinted from *Journal of lnvestigative Dermatology* (1963) 40, l-5.)

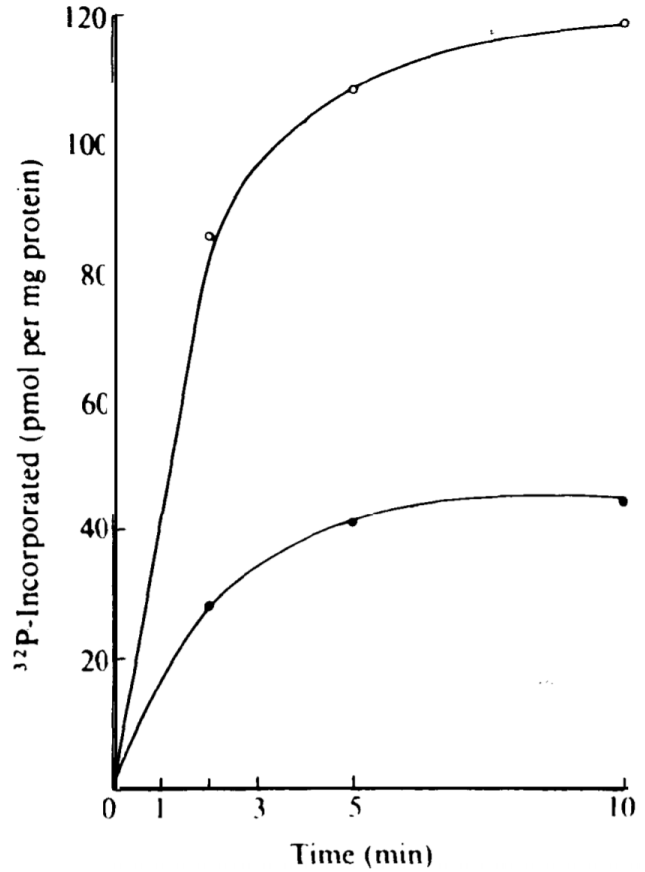

Figure 4. Stimulation of EGF of the incorporation of ^{32}P-hosphate from [γ-^{32}P] ATP into cell membranes. The reaction mixtures contained A-431 membrane (27 µg protein), HEPES buffer (20 mM, pH 7.4), MnCI, (1 mM), [γ-^{32}P]ATP (15 µM, 8X lO^{5}c.p.m.), EGF (40 ng) and BSA (7.5 µg) in a final volume of60 µ1. The reaction tubes were placed on ice and preincubated for 10 min in the presence (0) or absence (●) of EGF. The reaction was initiated by the addition of labelled ATP and incubation at 0°C was continued for the indicated times. The reaction was terminated by pipetting 50-µl aliquots on to squares (2 cm) of Whatman 3 MM filter paper and immediately dropping the paper into a beaker of cold 10% TCA containing 0.01 M sodium pyrophosphate. The filter papers were washed extensively with pyrophosphate-containing 10% TCA at room temperature, extracted with alcohol and ether dried, and the radioactivity measured in a Nuclear Chicago gas-flow counter. (reprinted from *Nature* (1978) 276, 408-410.)

Stanley Cohen, Nobel Prize Lecture 1986

First experiments demonstrating polyoma middle T and v-Src tyrosine kinase activity

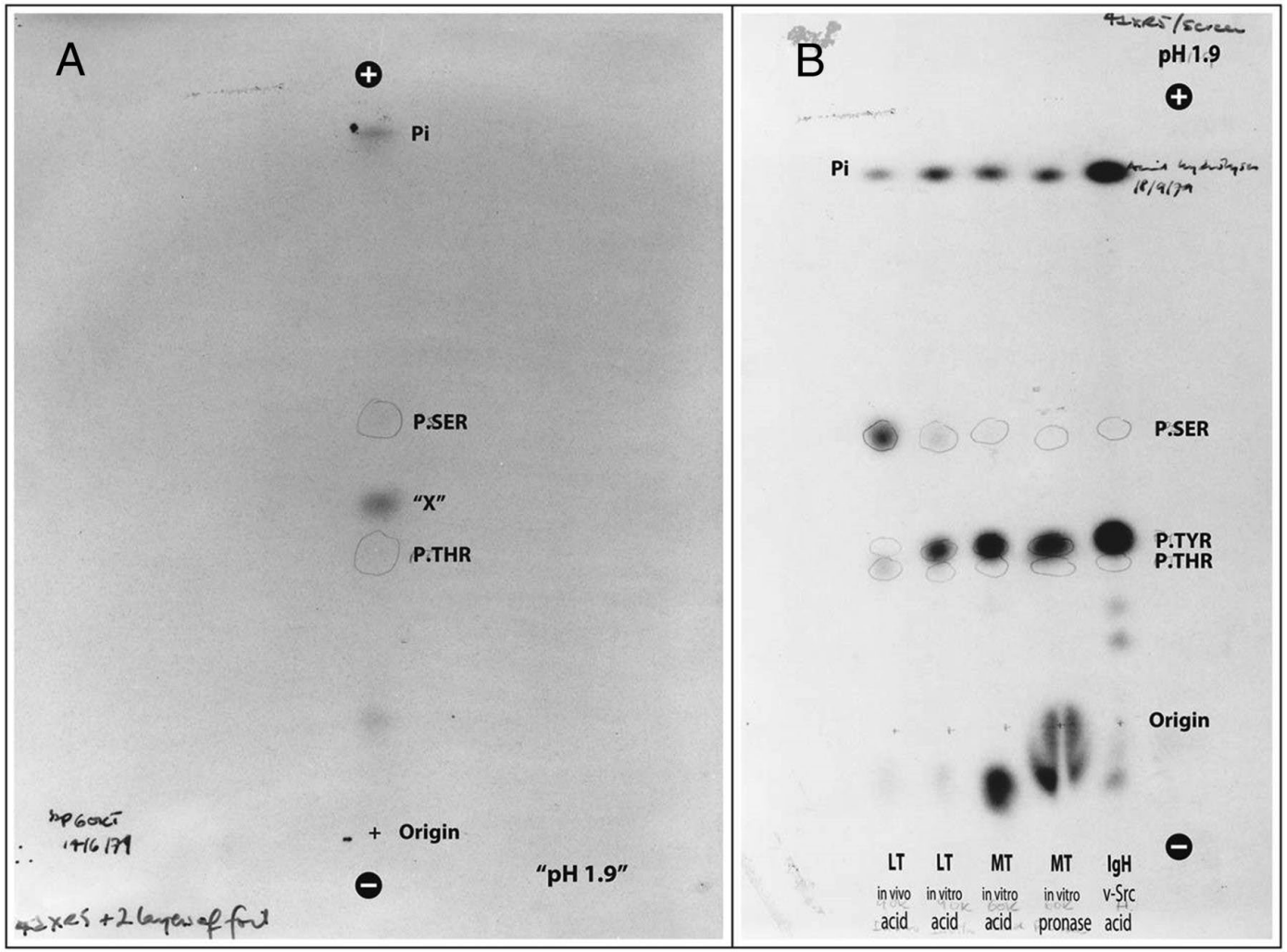

Tony Hunter PNAS 2015;112:26:7877-7882

PNAS

Humans have 58 known RTKs (20 subfamilies)

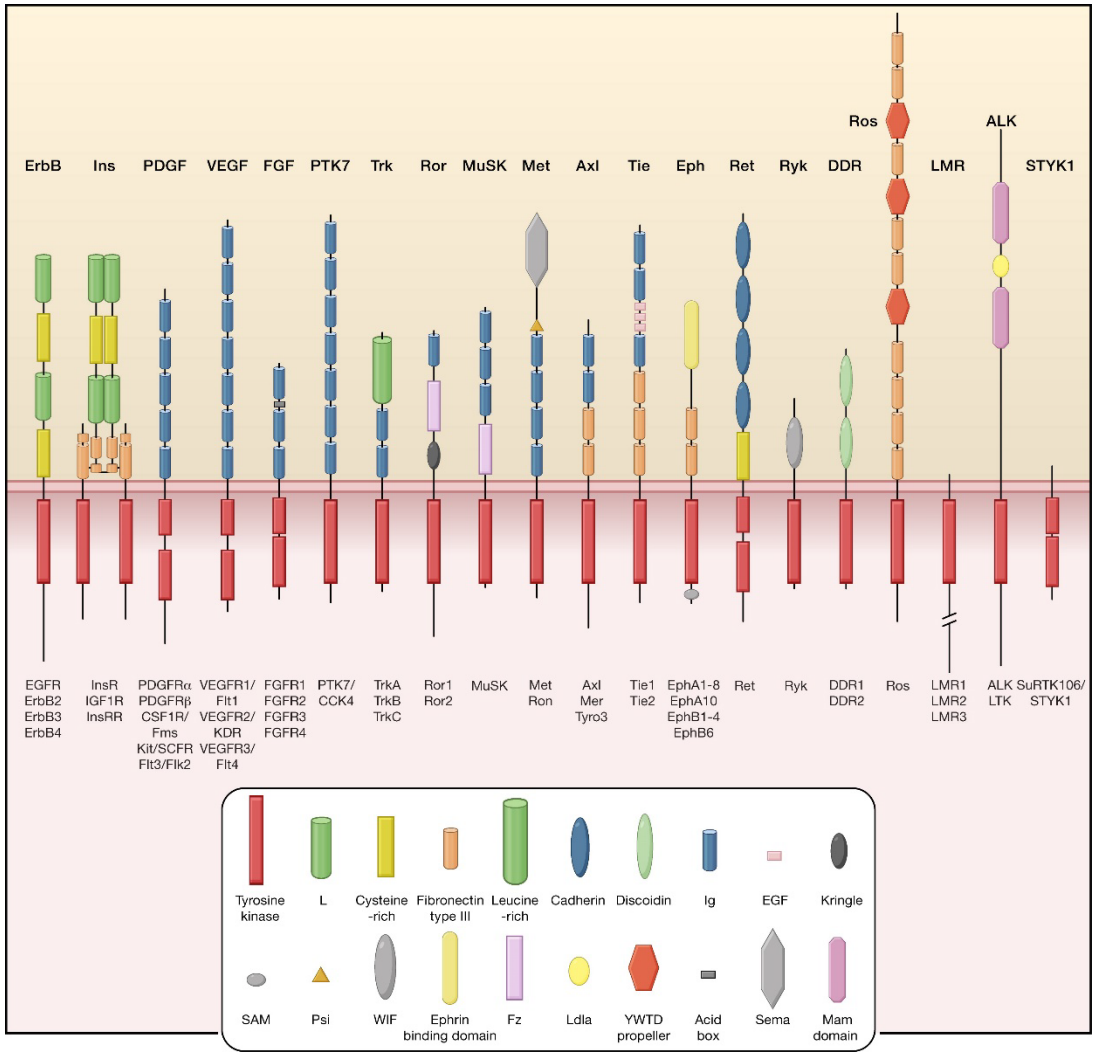

RTK Dimerization and Kinase Activation

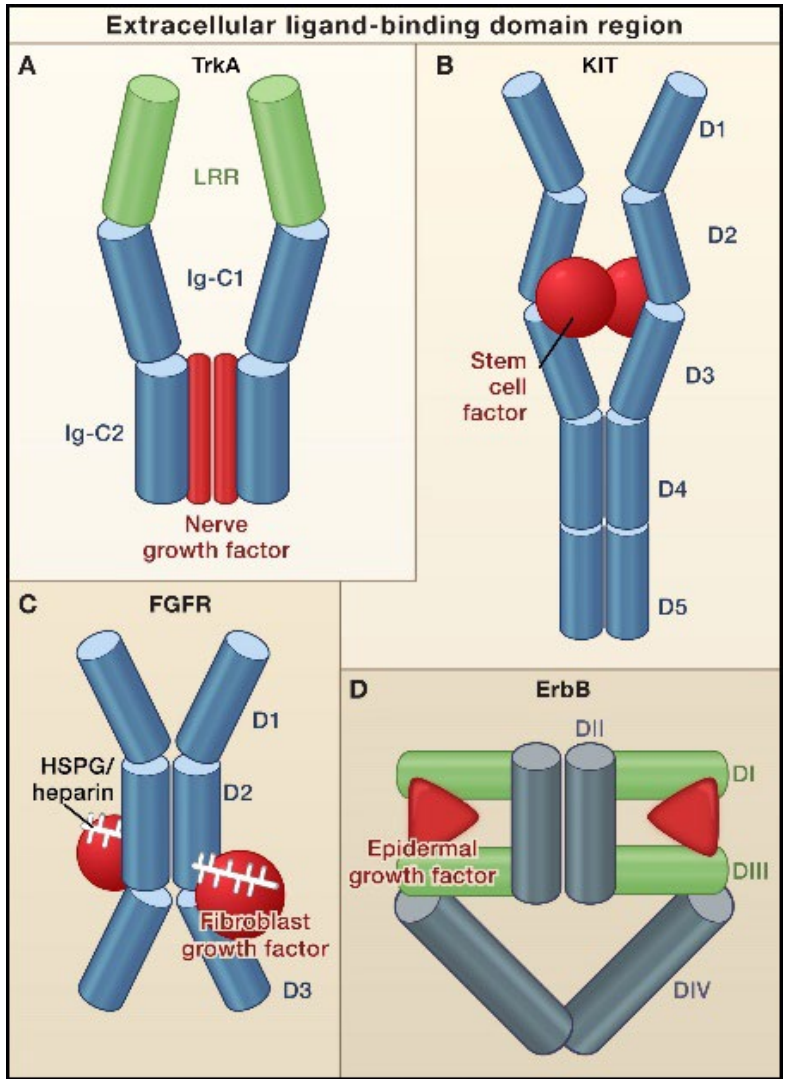

- Receptor activation requires dimerization/oligomerization
- Ligand-mediated dimerization
  - TrkA
- Ligand- and receptor-mediated dimerization
  - KiIT
  - FGFR
- Receptor-mediated dimerization
  - ErbB

RTK Dimerization and Kinase Activation

- Tyrosine kinase domain architecture: Each TKD is *cis*-autoinhibited and release of autoinhibition required for activity
  - N lobe
  - C lobe
  - Activation loop or other mechanism
- Mechanism for activation of kinase can differ

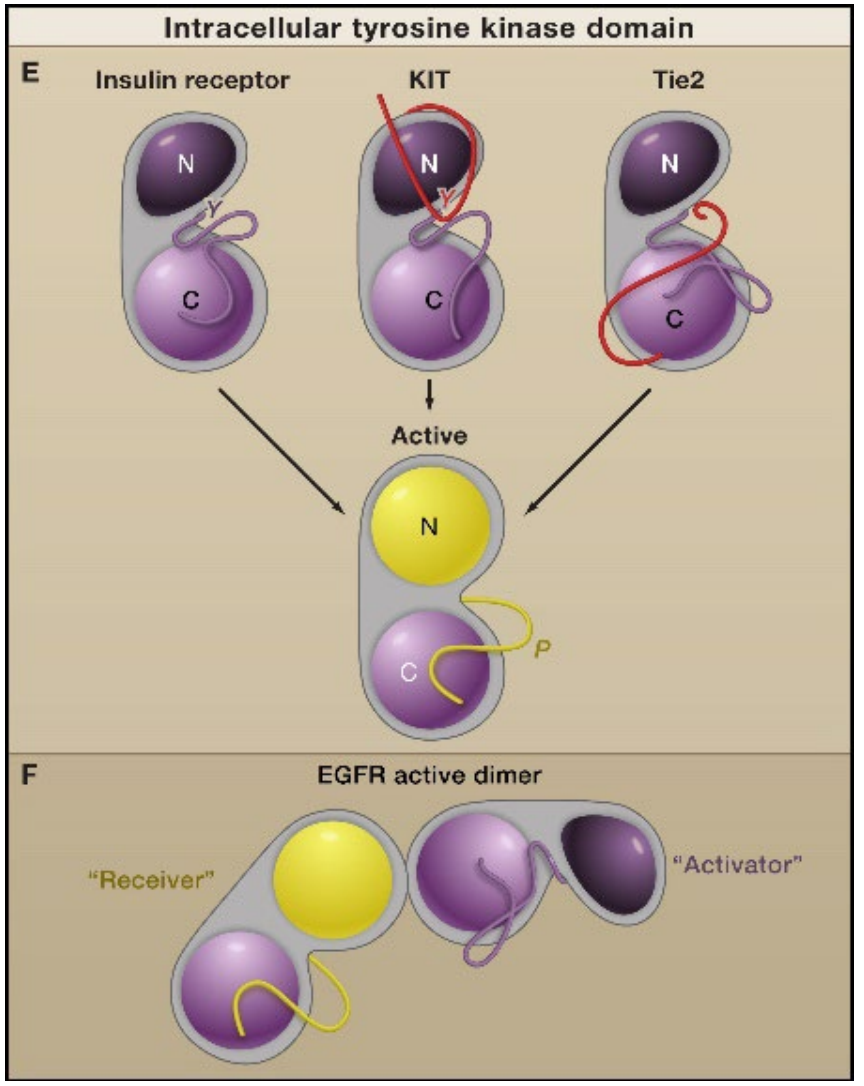

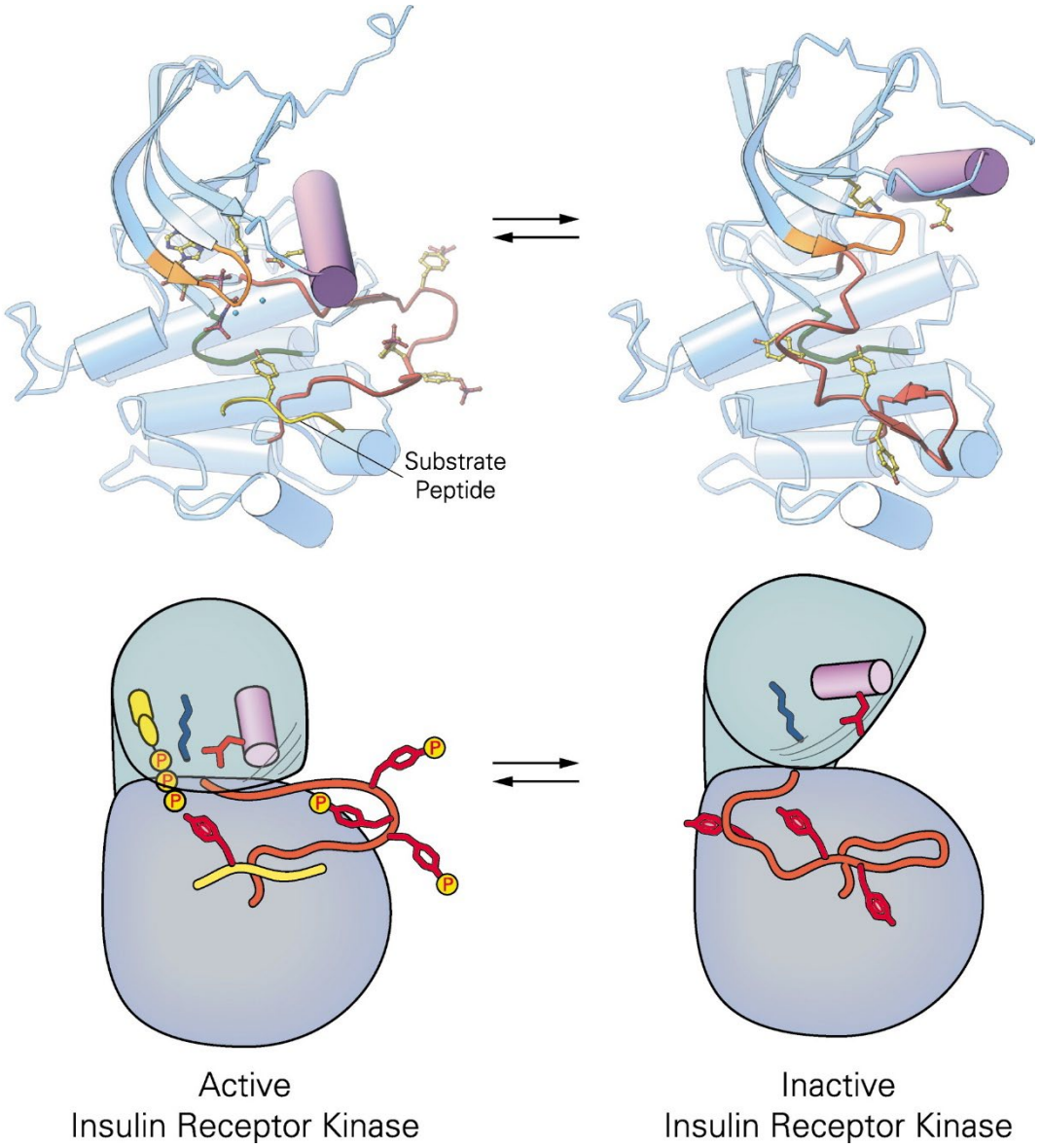

- N-lobe is composed of five-stranded β-sheet and one helix αC
- C-lobe predominantly helical
- ATP bound between the lobes with a GXGXϕG phosphate binding loop
- Activation loop provides platform for binding peptide substrate
- Catalytic lysine and glutamate are present in the N-lobe

Cell 2002 109, 275-282DOI: (10.1016/S0092-8674(02)00741-9)

RTK Signaling through adapter proteins

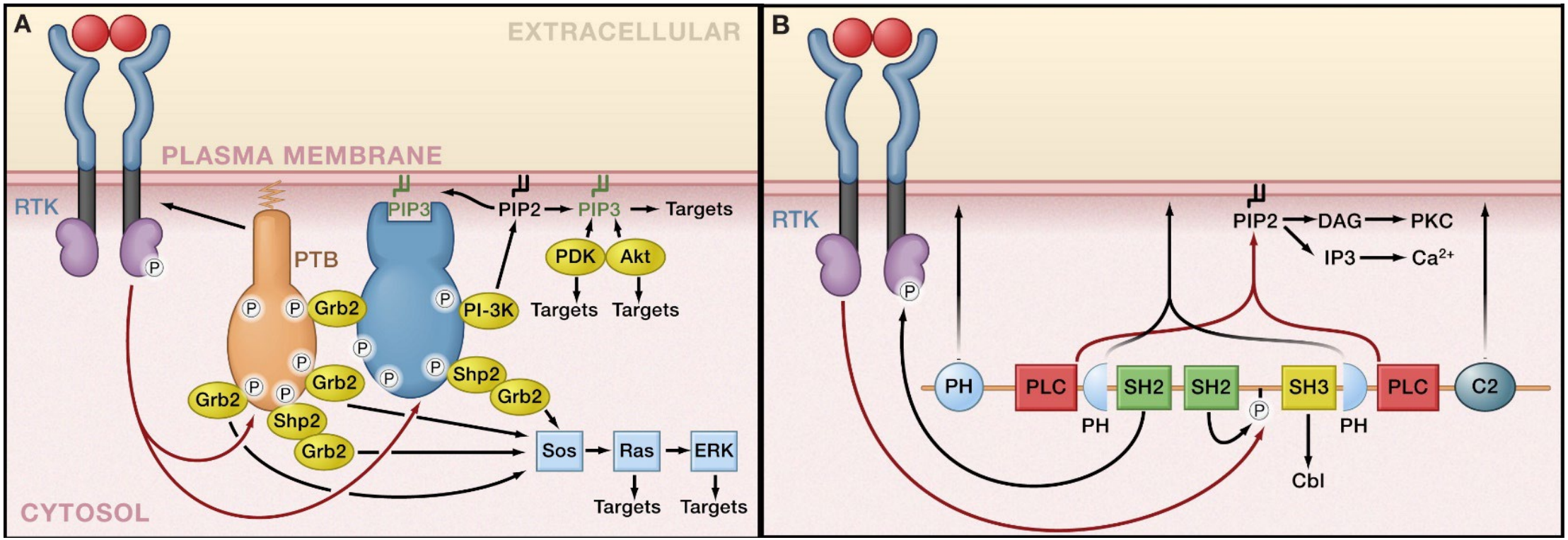

PTB – phosphotyrosine binding domain; SH2 domain – binds to phosphorylated tyrosines

EGF receptor signaling

"Bow-tie" network for RTK integration

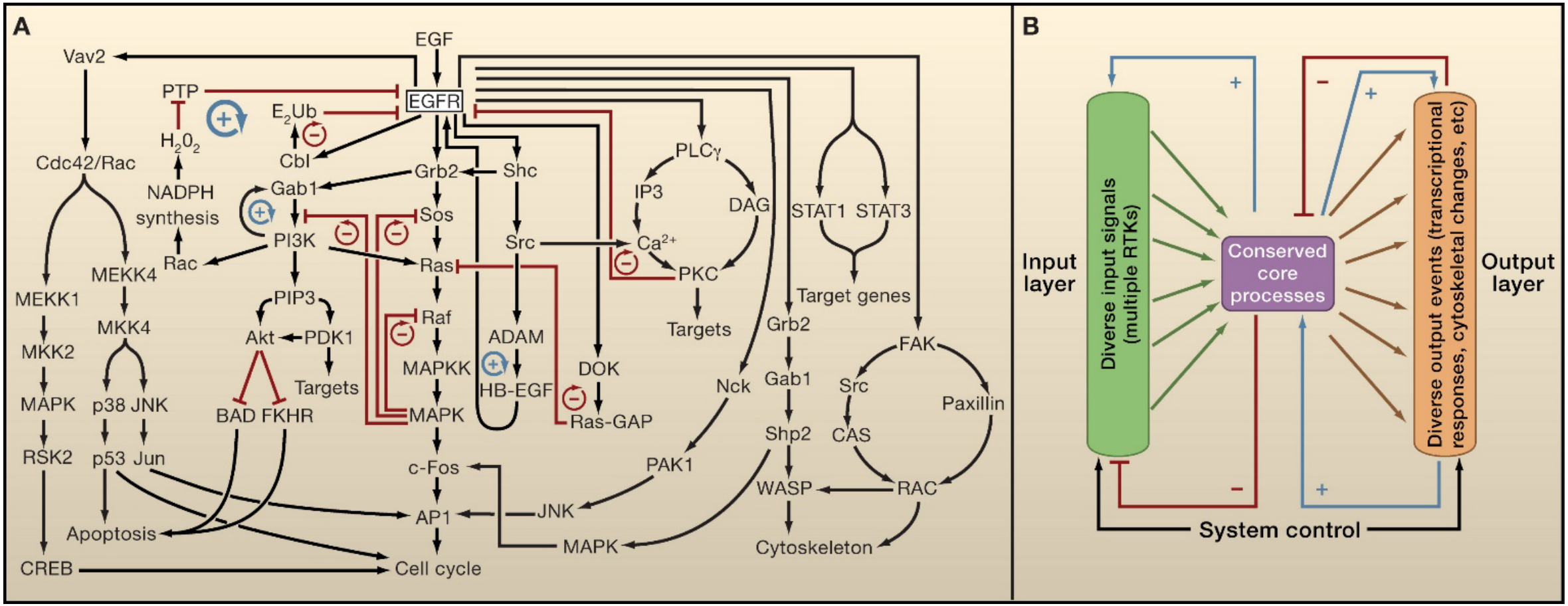

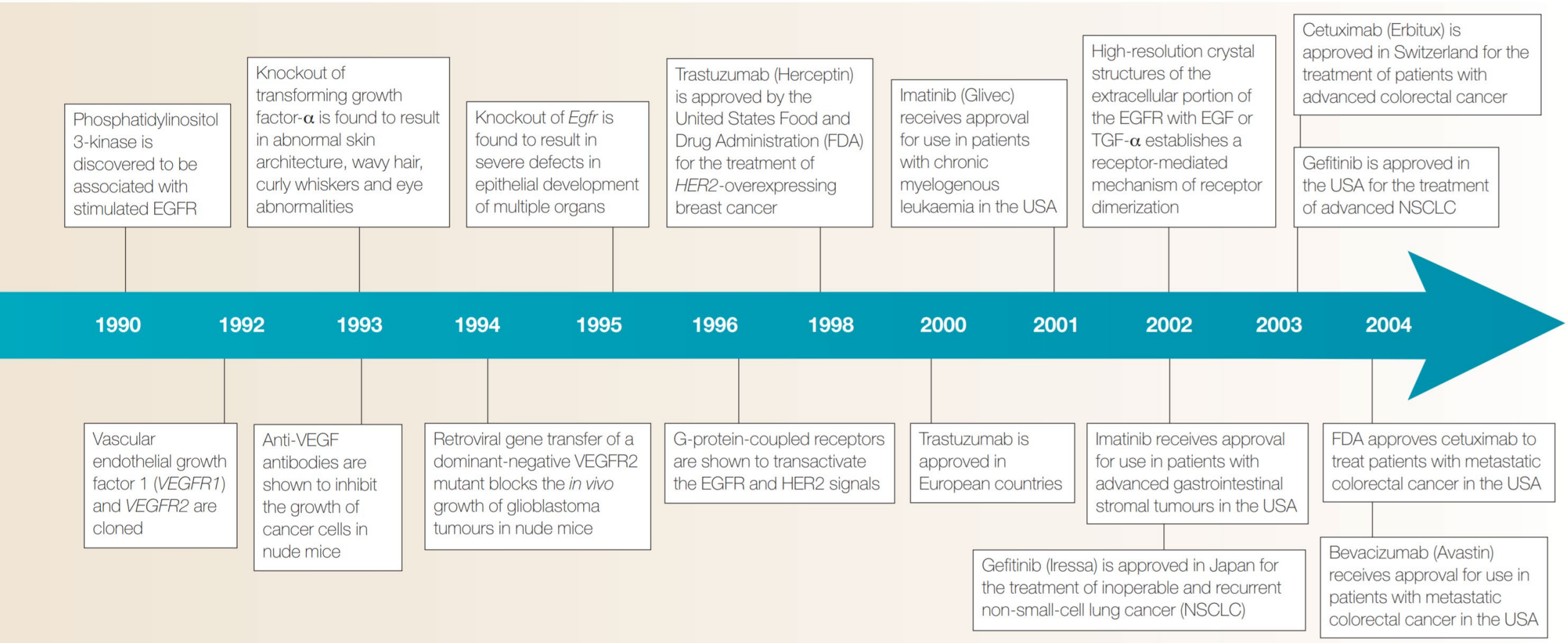
1990
Phosphatidylinositol 3-kinase is discovered to be associated with stimulated EGFR
1992
Vascular endothelial growth factor 1 (*VEGFR1*) and *VEGFR2* are cloned
1993
Knockout of transforming growth factor-α is found to result in abnormal skin architecture, wavy hair, curly whiskers and eye abnormalities
Anti-VEGF antibodies are shown to inhibit the growth of cancer cells in nude mice
1994
Knockout of *Egfr* is found to result in severe defects in epithelial development of multiple organs
Retroviral gene transfer of a dominant-negative VEGFR2 mutant blocks the *in vivo* growth of glioblastoma tumours in nude mice
1995
1996
Trastuzumab (Herceptin) is approved by the United States Food and Drug Administration (FDA) for the treatment of *HER2*-overexpressing breast cancer
G-protein-coupled receptors are shown to transactivate the EGFR and HER2 signals
1998
2000
Imatinib (Glivec) receives approval for use in patients with chronic myelogenous leukaemia in the USA
Trastuzumab is approved in European countries
2001
2002
High-resolution crystal structures of the extracellular portion of the EGFR with EGF or TGF-α establishes a receptor-mediated mechanism of receptor dimerization
Imatinib receives approval for use in patients with advanced gastrointestinal stromal tumours in the USA
Gefitinib (Iressa) is approved in Japan for the treatment of inoperable and recurrent non-small-cell lung cancer (NSCLC)
2003
Gefitinib is approved in the USA for the treatment of advanced NSCLC
2004
Cetuximab (Erbitux) is approved in Switzerland for the treatment of patients with advanced colorectal cancer
FDA approves cetuximab to treat patients with metastatic colorectal cancer in the USA
Bevacizumab (Avastin) receives approval for use in patients with metastatic colorectal cancer in the USA

Imatinib (ok – it actually targets a non-receptor tyrosine kinase)

- Chronic myelogenous leukemia – Nowell and Hungerford show an abnormal chromosome (Philadelphia chromosome)
- Rowley shows it is due to translocation
- Later shown to result in a fusion protein BCR-ABL
- BCR-ABL protein promotes abnormal WBC proliferation

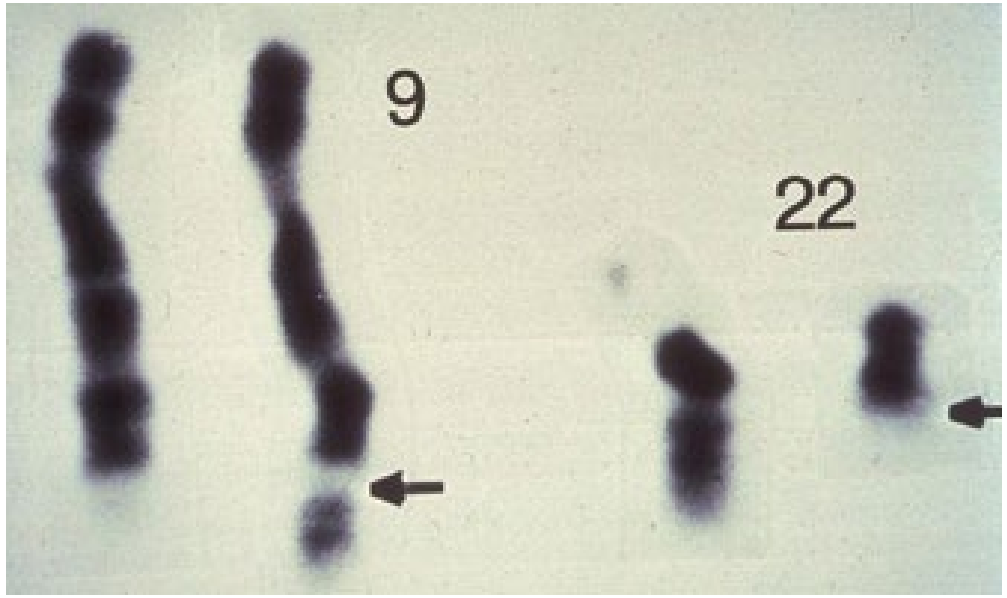

https://www.nature.com/scitable/topicpage/gleevec-the-breakthrough-in-cancer-treatment-565/

Imatinib (ok – it actually targets a non-receptor tyrosine kinase)

- Brian Druker collaborated with Ciba-Geigy (now Novartis) to screen their kinase inhibitors
- Identified a compound which inhibited BCR-ABL and tumor growth *in vitro*
- > 90% response *in vivo*, ushering in the era of targeted therapies

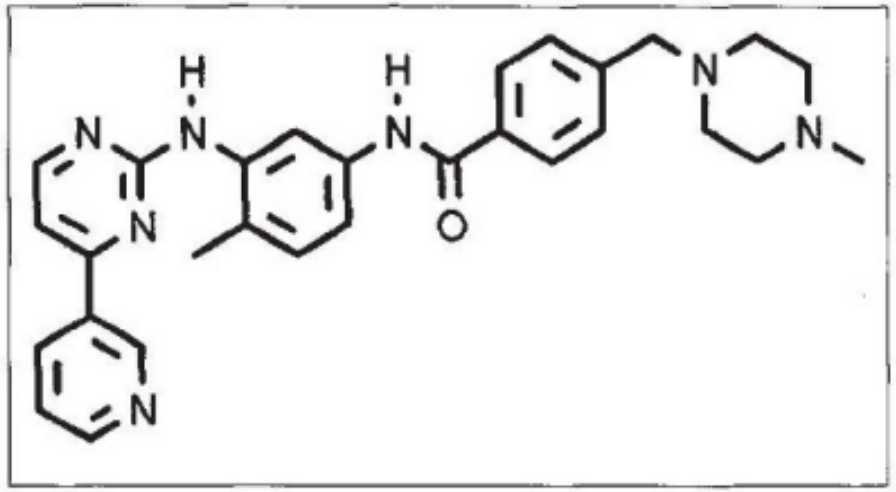

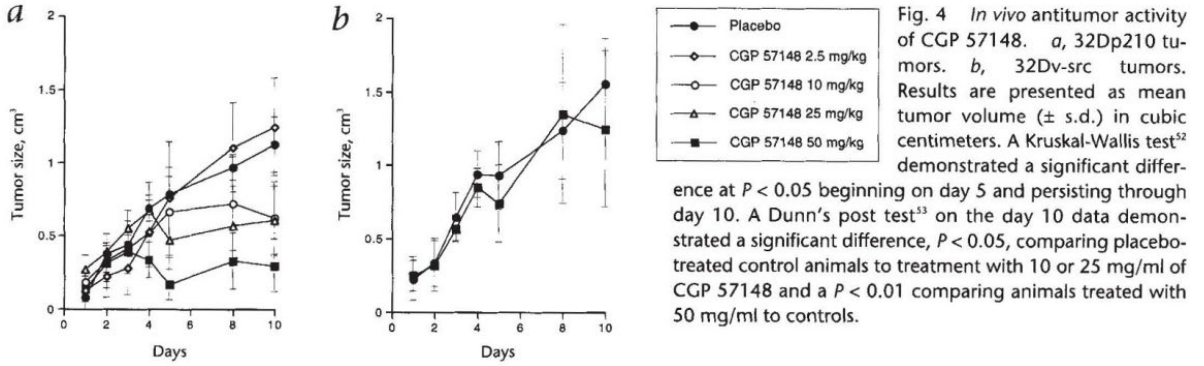

Fig. 4 *In vivo* antitumor activity of CGP 57148. *a*, 32Dp210 tumors. *b*, 32Dv-src tumors. Results are presented as mean tumor volume (± s.d.) in cubic centimeters. A Kruskal-Wallis test[52] demonstrated a significant difference at $P < 0.05$ beginning on day 5 and persisting through day 10. A Dunn's post test[53] on the day 10 data demonstrated a significant difference, $P < 0.05$, comparing placebo-treated control animals to treatment with 10 or 25 mg/ml of CGP 57148 and a $P < 0.01$ comparing animals treated with 50 mg/ml to controls.

Nature Medicine volume 2, pages 561–566 (1996)

Cancer Therapies

Target	Compound	Cancer	References
EGFR family			
HER2	Trastuzumab (Herceptin)	HER2-positive breast cancer	[7–9]
EGFR	Cetuximab (Erbitux)	Metastatic colorectal cancer (RAS wild type)	[10]
	Panitumumab (Vectibix)		[10–12]
	Gefitinib (Iressa)	Metastatic non-small-cell lung cancer	[13–15]
	Erlotinib (Tarceva)		[13,16]
EGFR and HER2	Lapatinib (Tykerb)	HER2-positive breast cancer (Trastuzumab-resistant)	[14,17]
	Afatinib	NSCLC	[18–21]
		HER2-positive breast cancer	
VEGFR	Sorafenib (Nexavar)	Renal, liver and thyroid cancer	[22–24]
	Sunitinib (Sutent)	Renal cell cancer	[25,26]
		Gastrointestinal stromal tumor (GIST)	
	Bevacizumab (Avastin)	Metastatic colorectal carcinoma	[27]
PDGFR	Imatinib (Gleevec)	GIST (KIT+)	[28]
PDGFR and VEGFR	Sunitinib	Angiogenesis	[29–32]
	Soratinib		
	Pazopanib		
	Nilotinib		
FGFR and VEGFR	Brivanib (BMS-540215)	Human hepatocellular carcinoma model	[33]
VEGFR, PDGFR, FLT-3, c-KIT and FGFR	CHIR-258 (TKI-258)	Multiple myelomas	[34,35]
MET	SGX523	MDCK and A549 cells and GTL16 xenograft models	[36]
C-KIT	Imatinib (Gleevec)	GIST	[37–39]

EGFR mutation+ response to TKIs

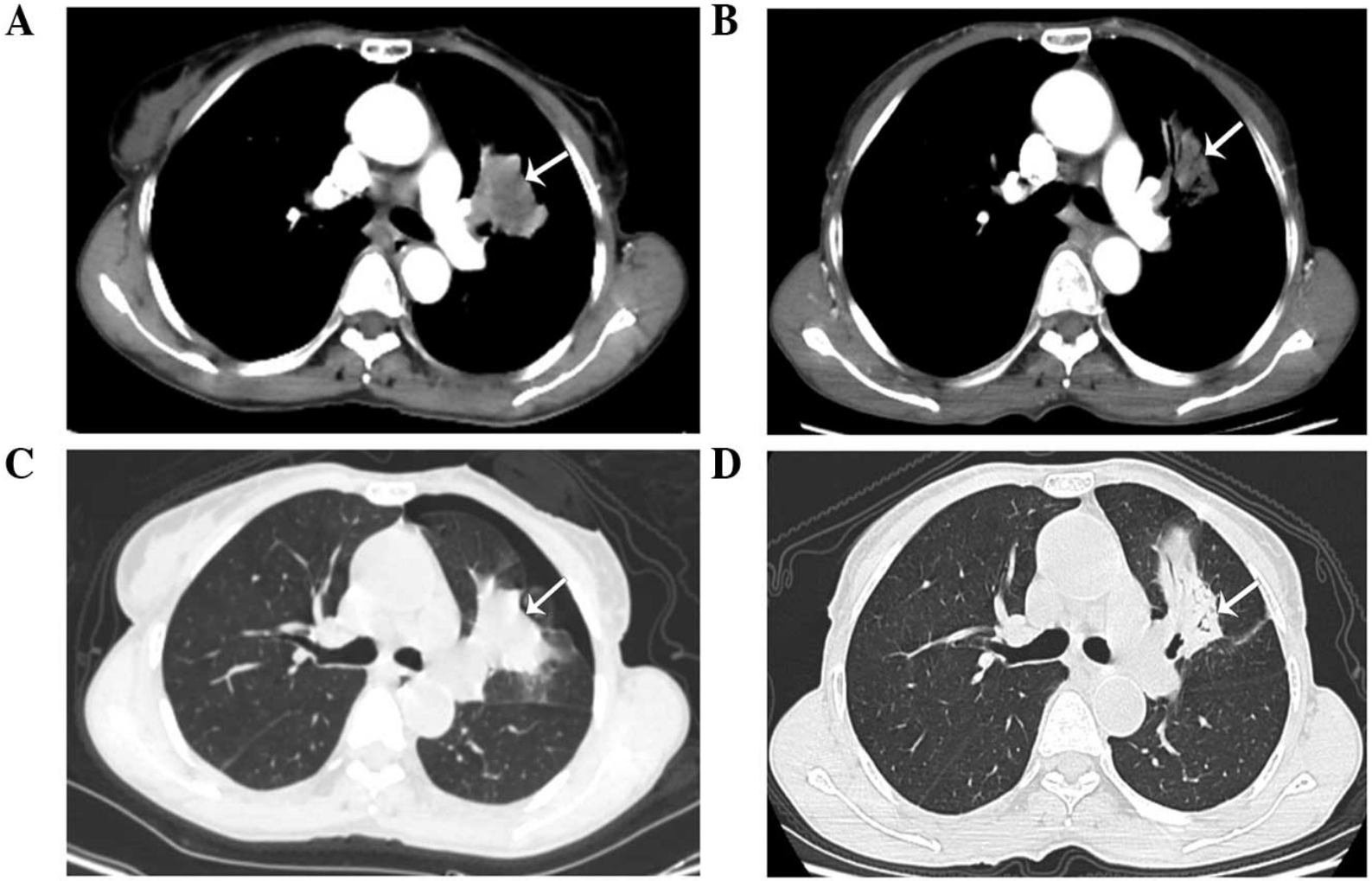

https://doi.org/10.3892/ol.2016.4409

Receptor Serine/Threonine Kinases

A summary of biological responses to TGFβ family signaling in development

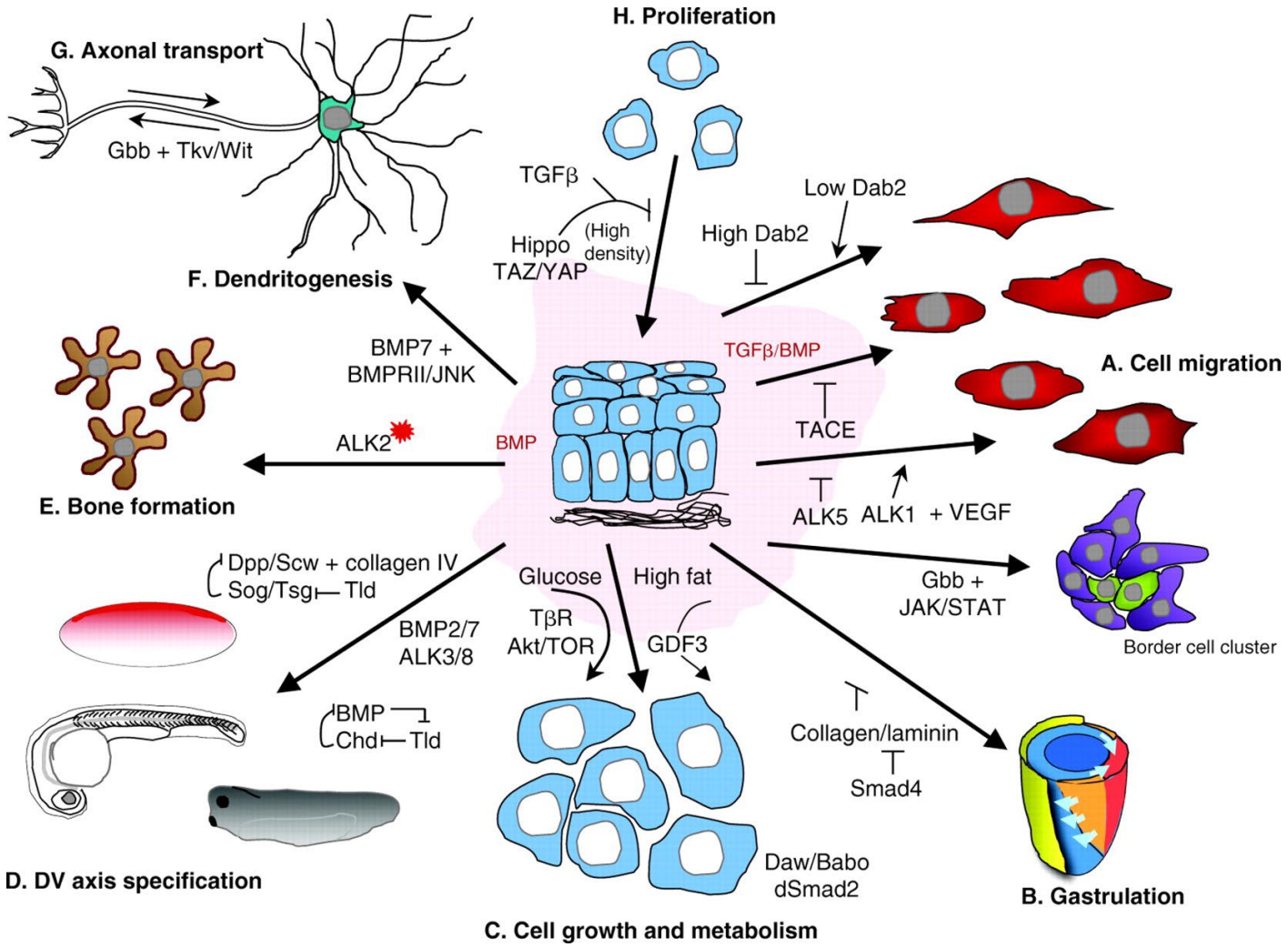

Kristi Wharton, and Rik Derynck Development 2009;136:3691-3697

Isolation of Tranforming Growth Factors

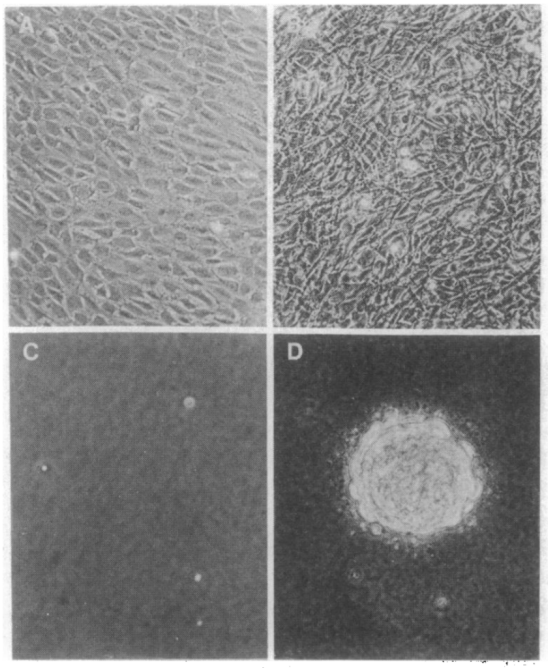

FIG. 2. Effect of SGFs on morphology and growth in soft agar. (*A*) Rat clone 49F seeded 6 days previously at 1×10^5 cells per 30-cm^2 tissue culture flask in Dulbecco's modified Eagle's medium containing 10% calf serum (the medium was changed once, 3 days after seeding). (*B*) Parallel culture treated with SGF (2.5 μg of protein per ml, fraction 43 from Fig. 1); the medium was changed 3 days after seeding and new SGF (fraction 43) was added. (*C*) Clone 49F cells at 2 weeks after seeding in soft agar without the addition of SGF. The cells were seeded at 1×10^4 cells per 20-cm^2 petri dish and were fed with a 2-ml overlay of 0.3% agar after 7 days. More than 10^7 rat fibroblast cells (clone 49F) have been plated in soft agar and, in the absence of SGFs, no spontaneous colony formation has been seen with this clone. (*D*) Cells in *C* except that 0.4 μg of protein from fraction 67 of Fig. 1 was incorporated per ml of the soft agar. After 1 week these cells were refed with 2 ml of 0.3% agar containing 0.4 μg of protein from the same fraction per ml. (*A*, ×45; *B*, ×45; *C*, ×90; *D*, ×90.)

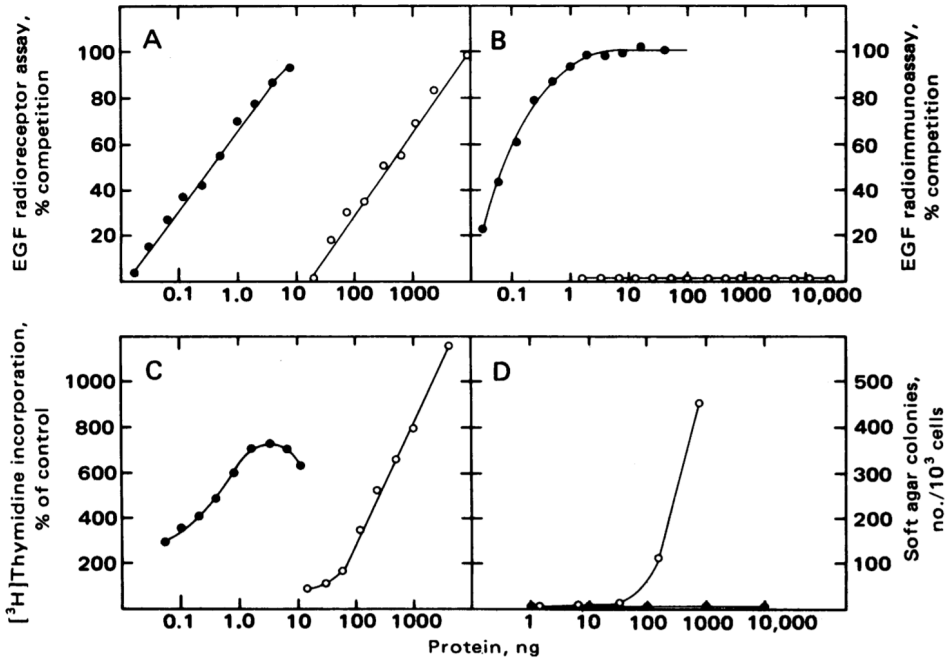

FIG. 3. Properties of EGF (●) and the 12,000 molecular weight peak of SGF (○) from Fig. 1. (*A*) EGF radioreceptor competition assays were performed with 2.5×10^4 mink lung cells and a sequential binding assay in which the competitor is allowed to preincubate with the cells at 22° for 1 hr. It is then removed, the cells are washed four times with binding buffer, and the ^{125}I-labeled EGF is incubated with the cells for 1 hr at 22°. (*B*) Radioimmunoassay using anti-EGF antibody and ^{125}I-labeled EGF. The antibody to mouse salivary gland EGF was produced in rabbits and the precipitating antibody was goat anti-rabbit IgG. (*C*) Thymidine incorporation studies using serum-depleted fibroblastic clone 49F. (*D*) Soft-agar growth-promoting activity. Rat clone 49F was seeded in the presence of varying concentrations of the peptides. The cells were fed 1 week after seeding and the colonies were counted at the end of 2 weeks.

De Larco and Todaro, Proc. Natl. Acad. Sci. USA 75 (1978)

Cloning of TβRs

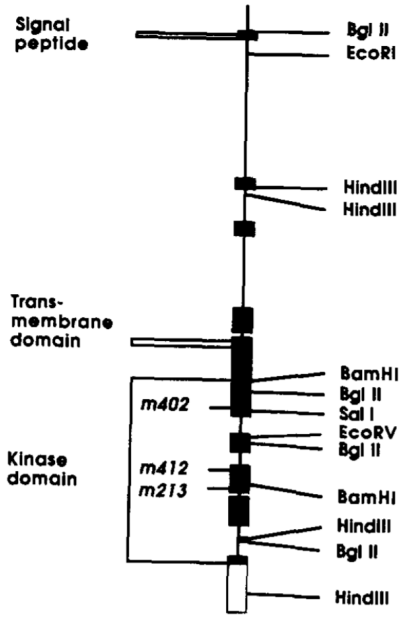

Figure 4. Physical Map of *daf-1*

A map based on restriction digests and sequence analysis of cDNA and genomic clones (see Figure 6) showing locations of 9 exons (solid boxes) and 8 introns. The open box represents the 3′ untranslated region of the transcript. The sites of Tc1 insertion in the mutant alleles were determined from restriction digests (Figure 3a) and by sequence analysis of cloned mutant DNA. Also shown is the location of a C to T transition resulting in a novel BglII site in the EMS-induced mutant allele *daf-1(m213)*. Evidence supporting the designation of protein functional domains (signal sequence, transmembrane and kinase domains) is provided in Figures 6–8.

Cell, Vol. 61, 635-645. May 18, 1990

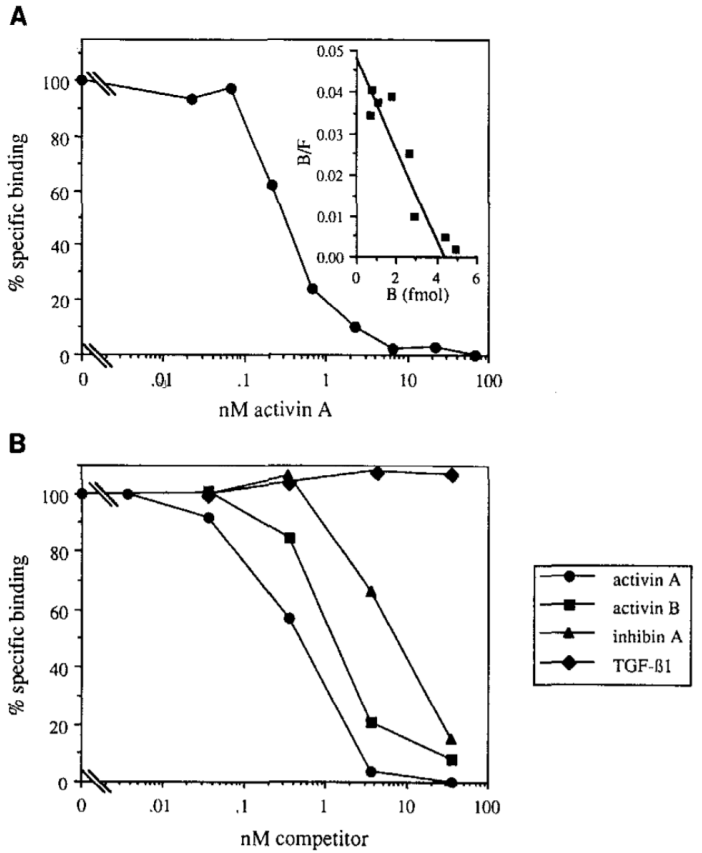

Figure 4. Competition Binding of ^{125}I-Activin A to COS Cells Transiently Transfected with pmActR1 or pmActR2

(A) ^{125}I-activin A binding to COS cells transfected with pmActR1. Binding was performed on cell monolayers as described in Experimental Procedures, and was competed with unlabeled activin A. Data are shown as percent specific binding, where 100% specific binding was 3.7% of input cpm and nonspecific binding was 0.9% of input cpm. Inset: Scatchard analysis of the data.

(B) ^{125}I-activin A binding to COS cells transfected with pmActR2. Binding was competed with unlabeled factors as indicated; 100% specific binding and nonspecific binding were 2.5% and 0.9%, respectively, of input cpm.

Cell, vol. 65, 973-982, June 14, 1991

TGF-β superfamily

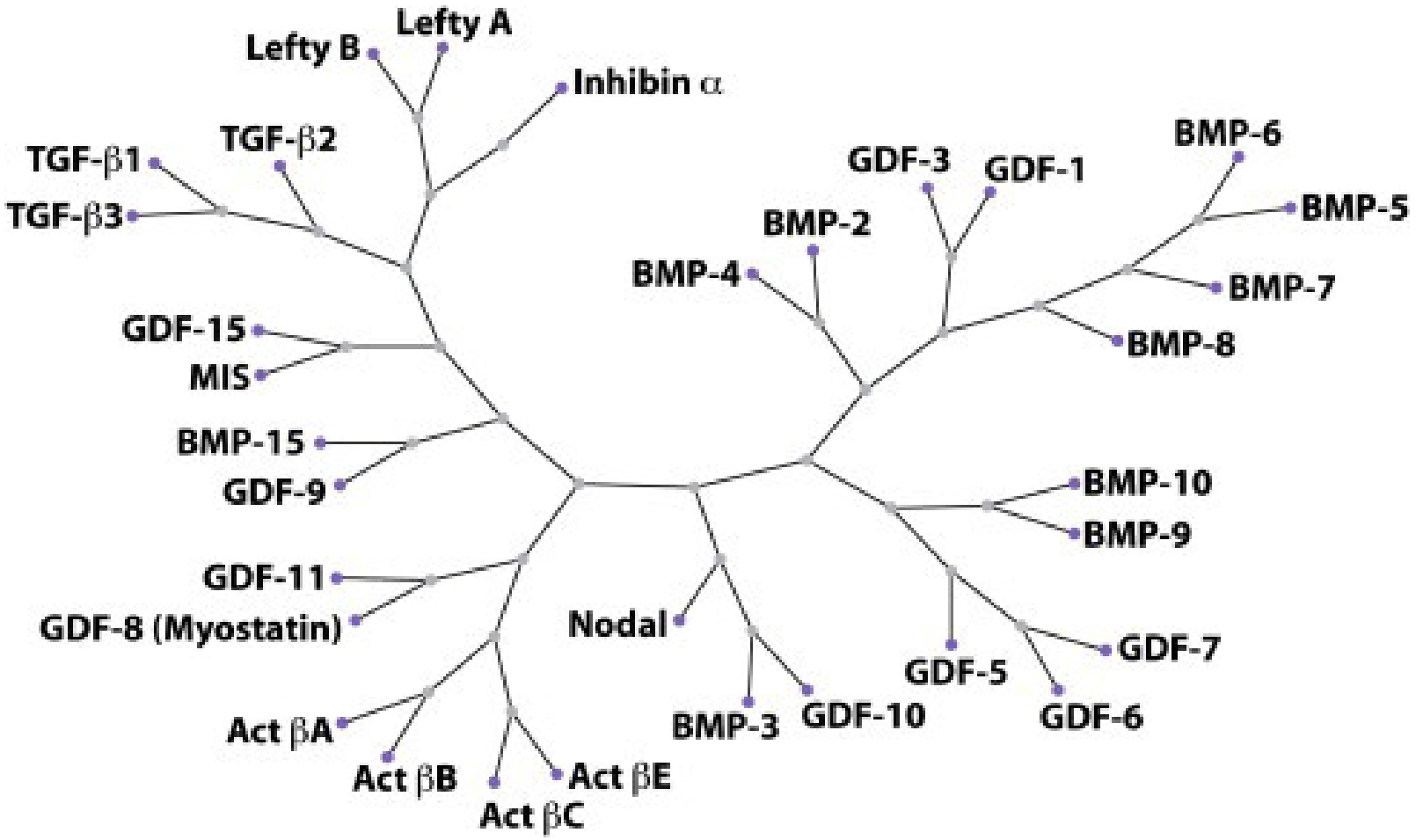

FEBS Letters, Volume: 586, Issue: 14, Pages: 1860-1870, First published: 28 May 2012, DOI: (10.1016/j.febslet.2012.05.028)

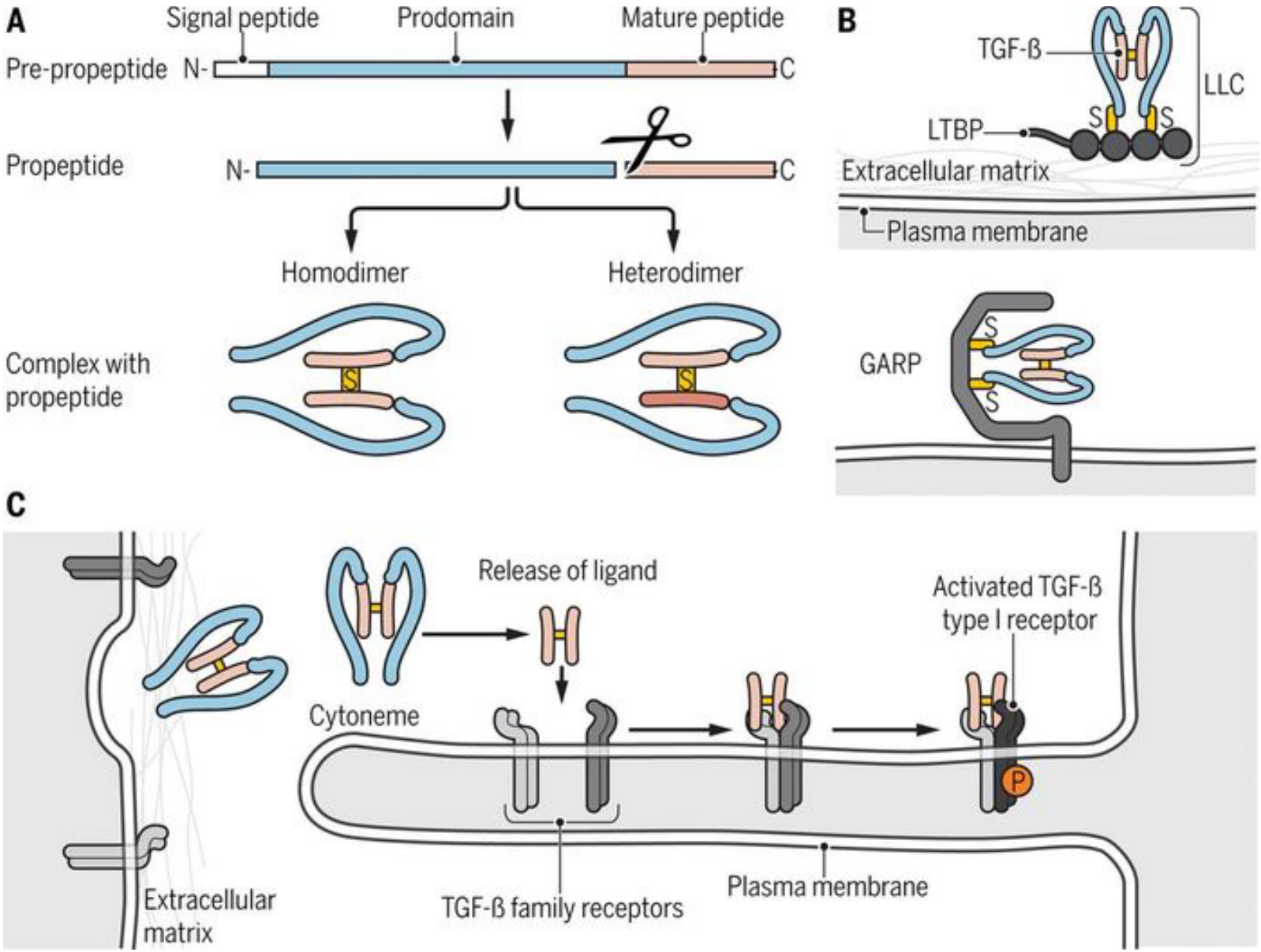

Specificity, versatility, and control of TGF-β family signaling, Volume: 12, Issue: 570, DOI: (10.1126/scisignal.aav5183)

Alternative modes of binding

Interunit disulfide and hydrophobic interactions stabilize the ligand dimer.

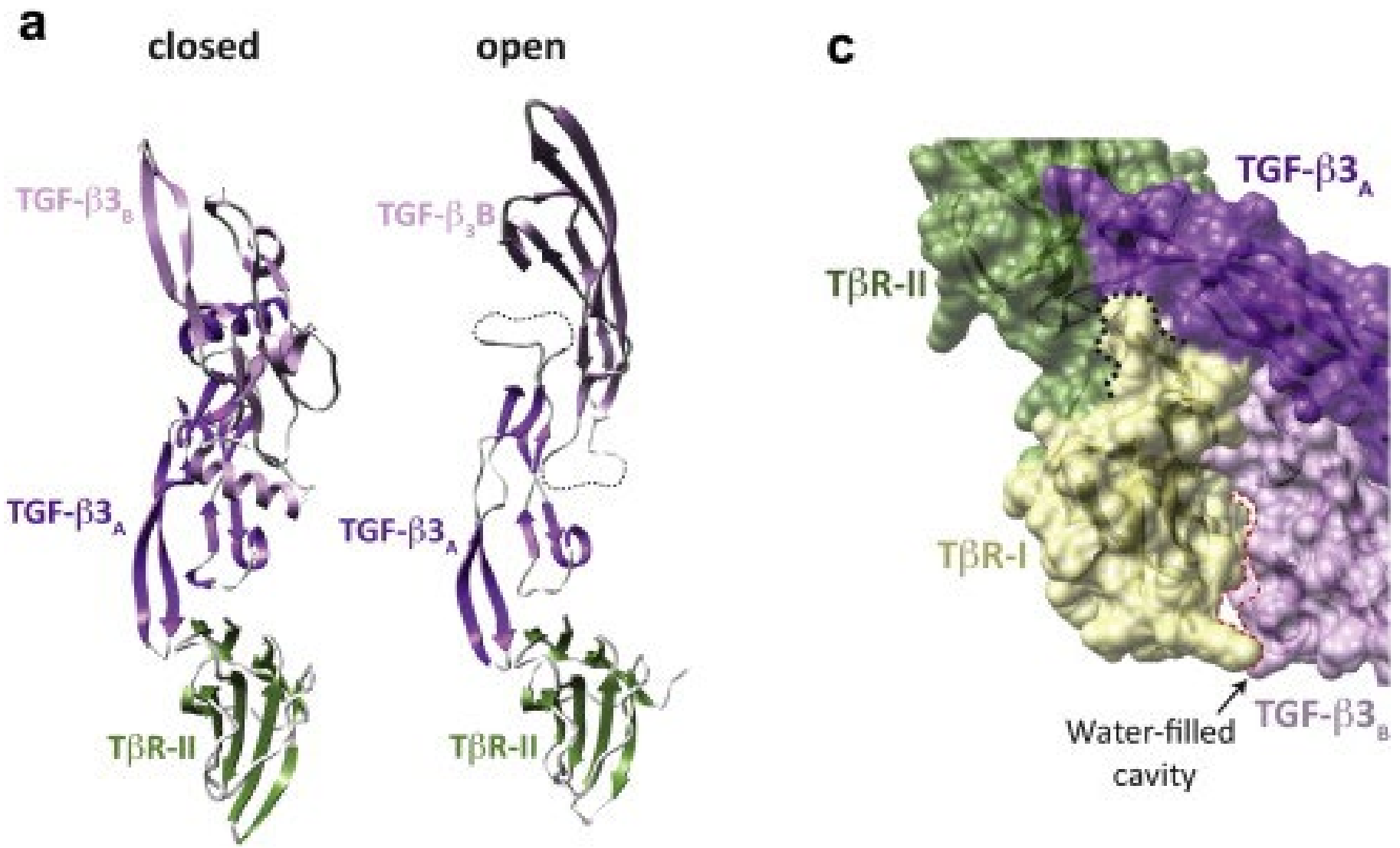

FEBS Letters, Volume: 586, Issue: 14, Pages: 1860-1870, First published: 28 May 2012, DOI: (10.1016/j.febslet.2012.05.028)

TGF-β dimerization and ligand traps

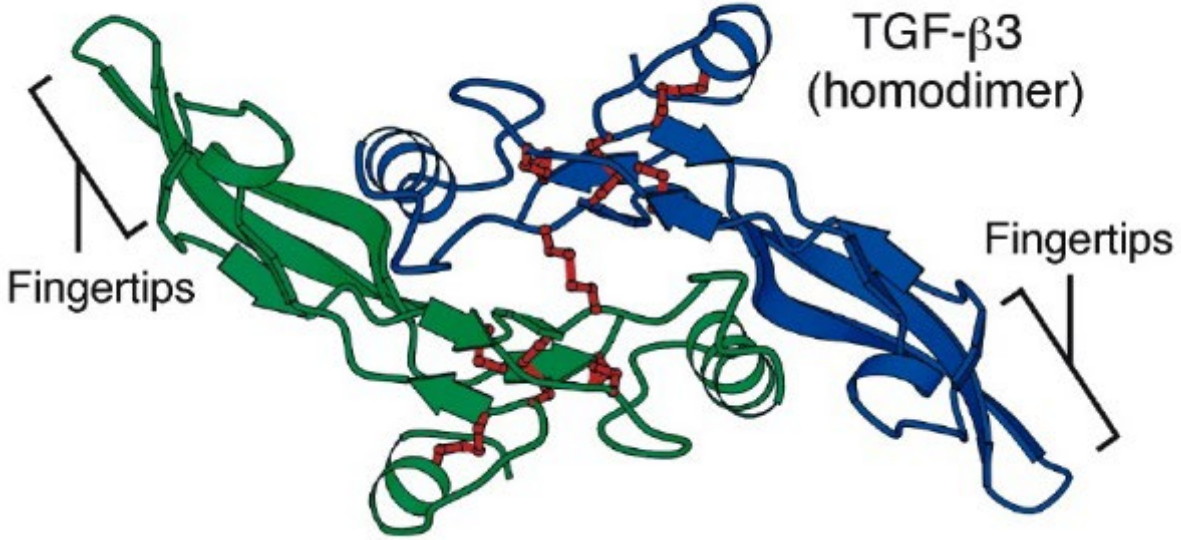

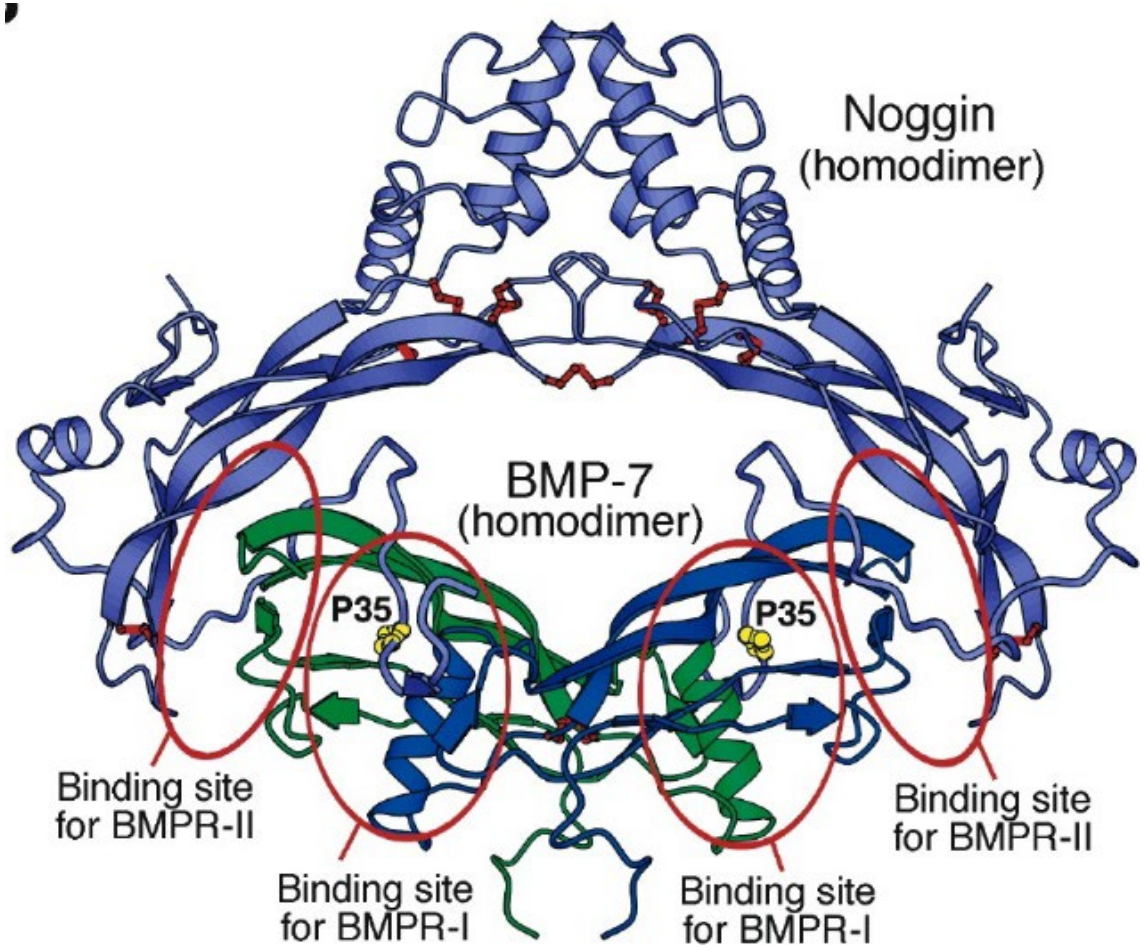

Cell, Vol. 113, 685–700, June 13, 2003

TGF-β superfamily, receptors and effectors

7 type I receptors
5 type II receptors

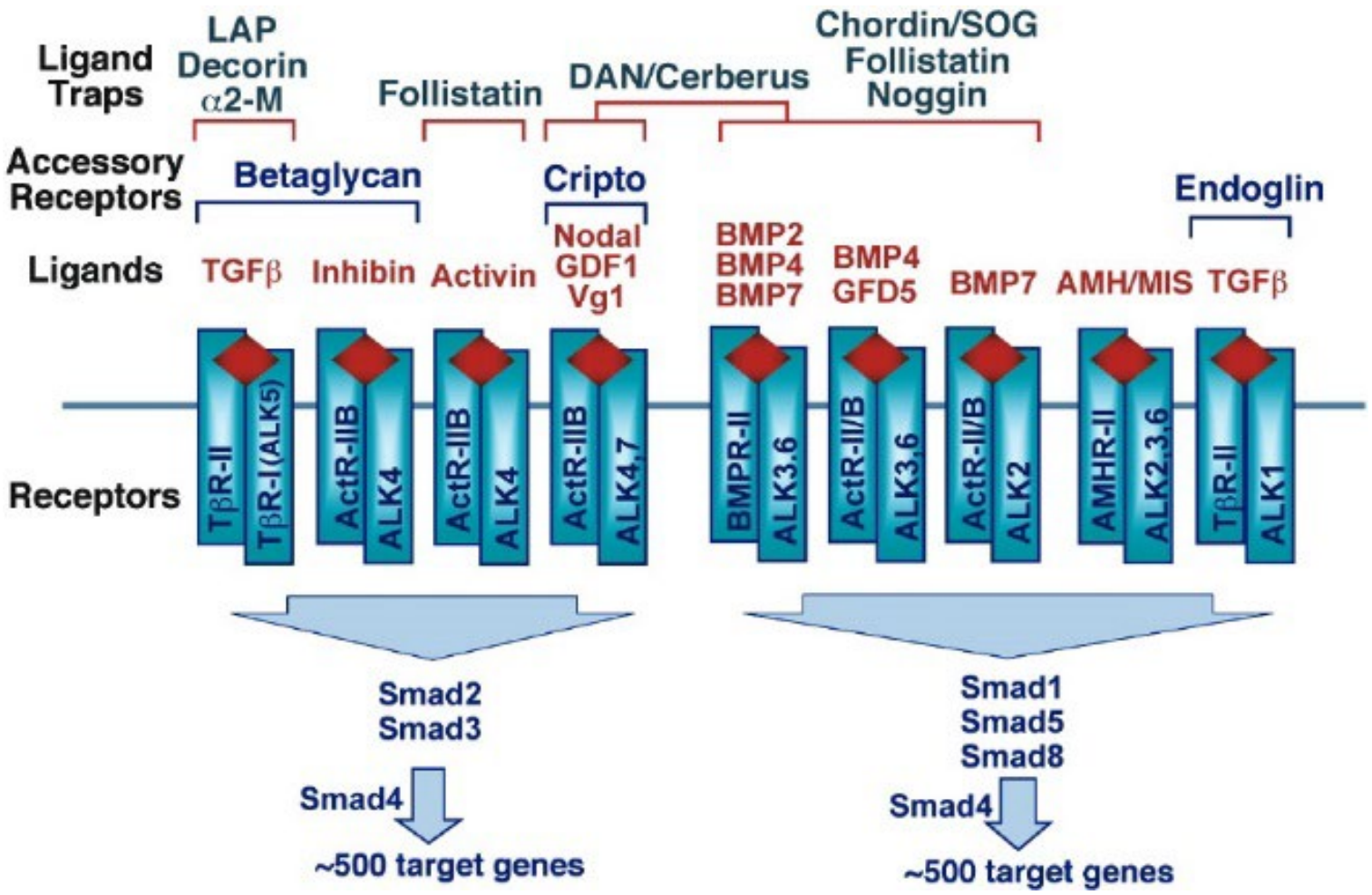

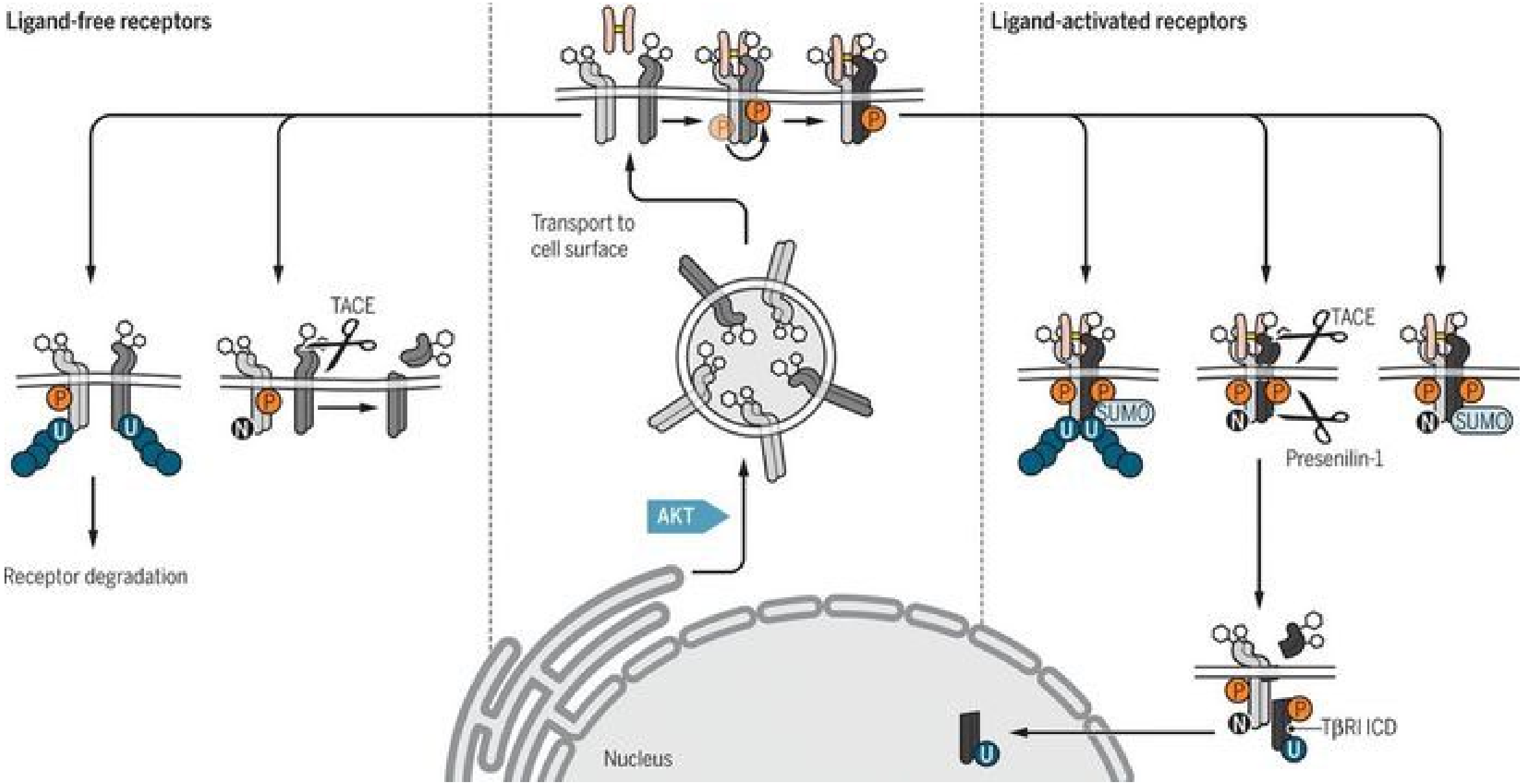

Specificity, versatility, and control of TGF-β family signaling, Volume: 12, Issue: 570, DOI: (10.1126/scisignal.aav5183)

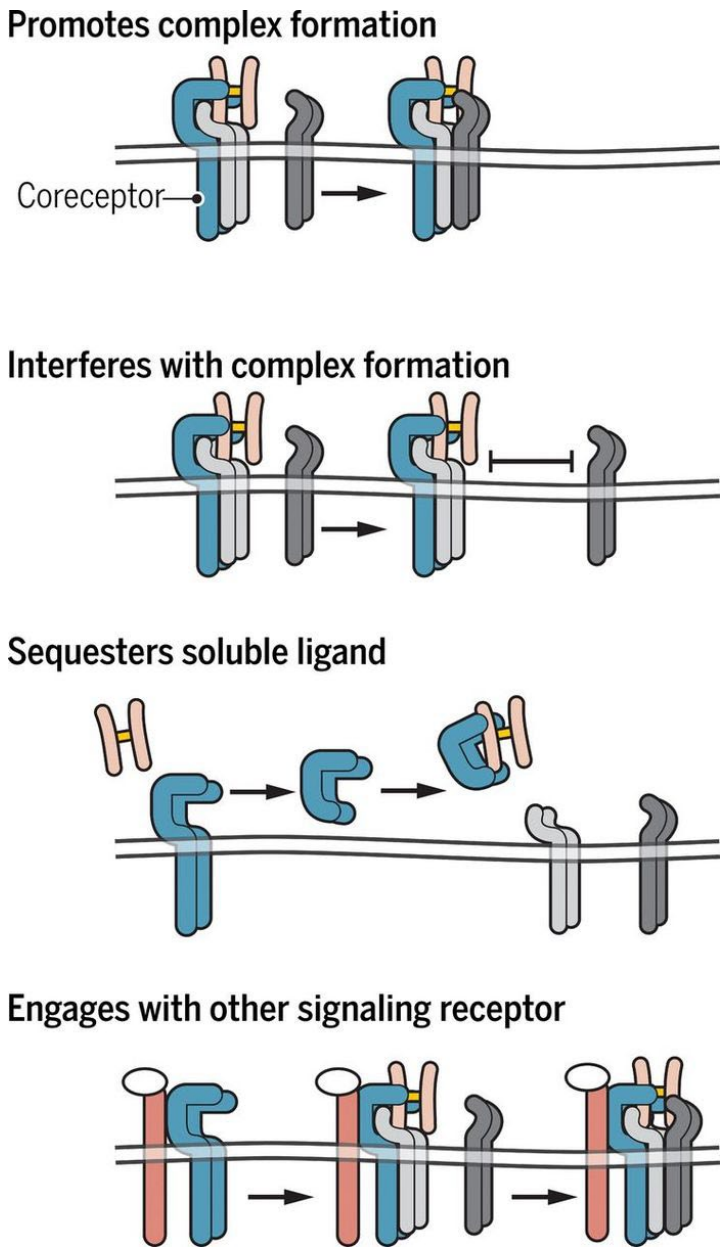

Specificity, versatility, and control of TGF-β family signaling, Volume: 12, Issue: 570, DOI: (10.1126/scisignal.aav5183)

TGF-β type I and type II receptors form a heterotetramer – TβRII activates TβRI kinase

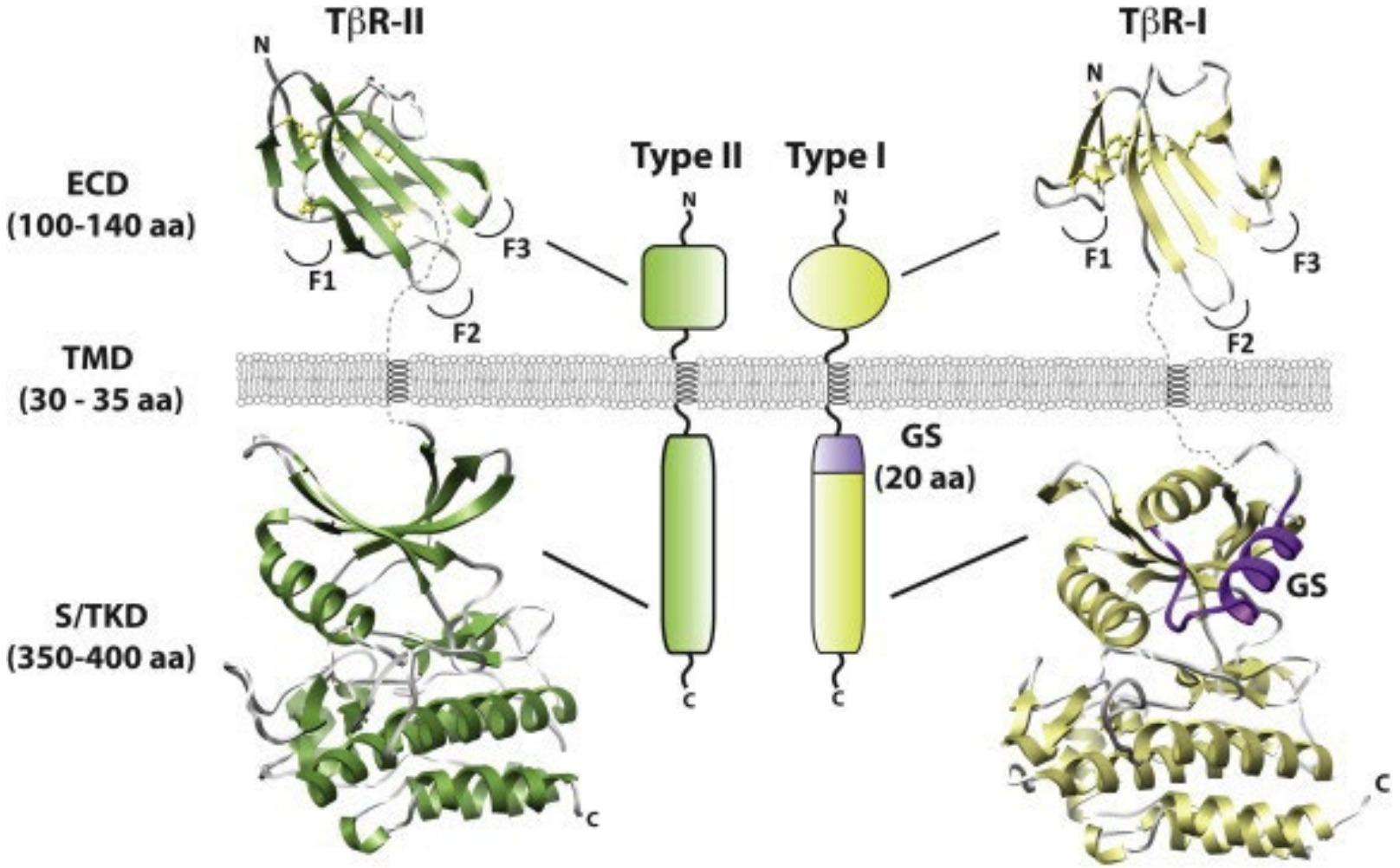

GS domain is phosphorylated by the type II receptor

FEBS Letters, Volume: 586, Issue: 14, Pages: 1860-1870, First published: 28 May 2012, DOI: (10.1016/j.febslet.2012.05.028)

Assembly of Ligand-Receptor Complexes

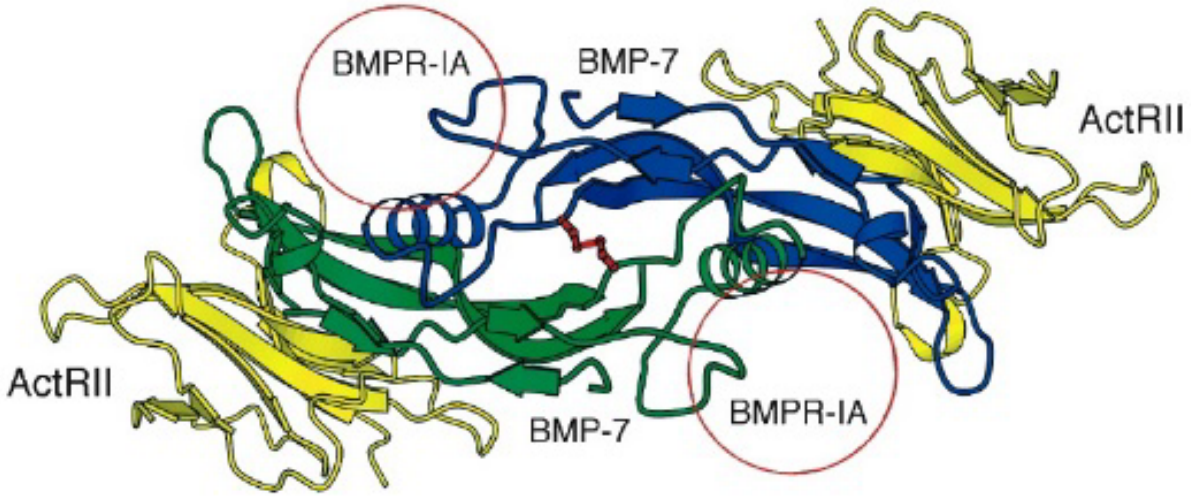

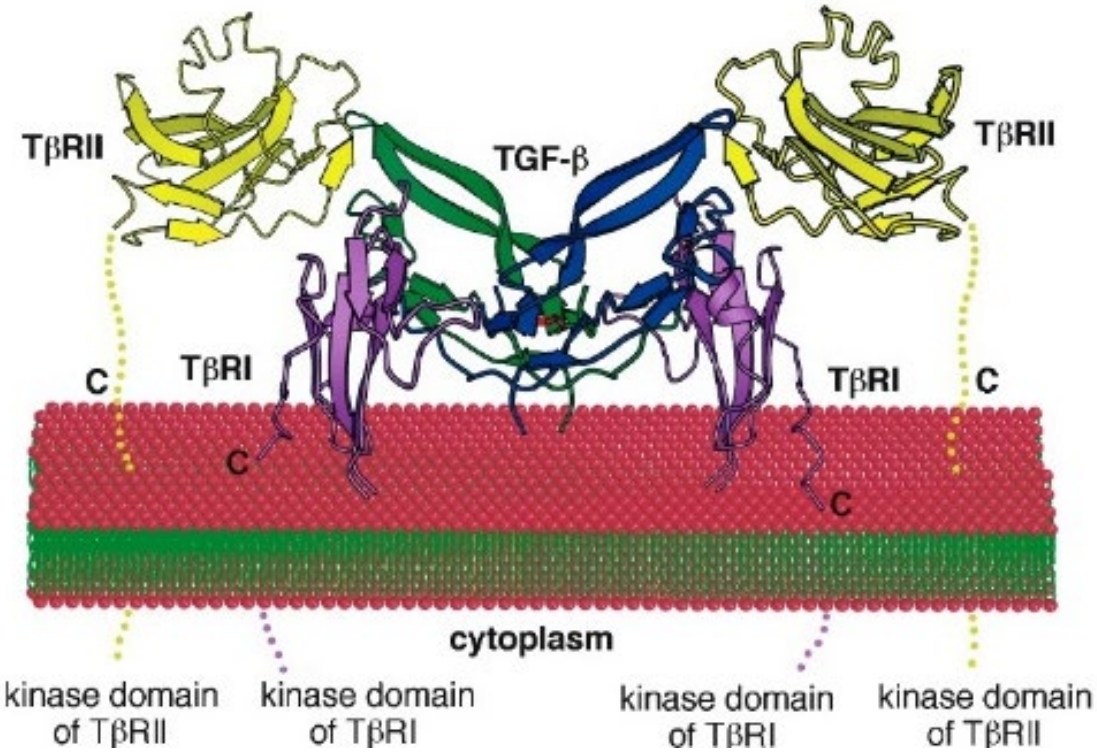

BMPs – bind to type I receptor first and then bind to type II receptor
TGF-β/Activins – bind to type II receptor first and then to type I

Cell, Vol. 113, 685–700, June 13, 2003

Regulation of S/T kinase activity

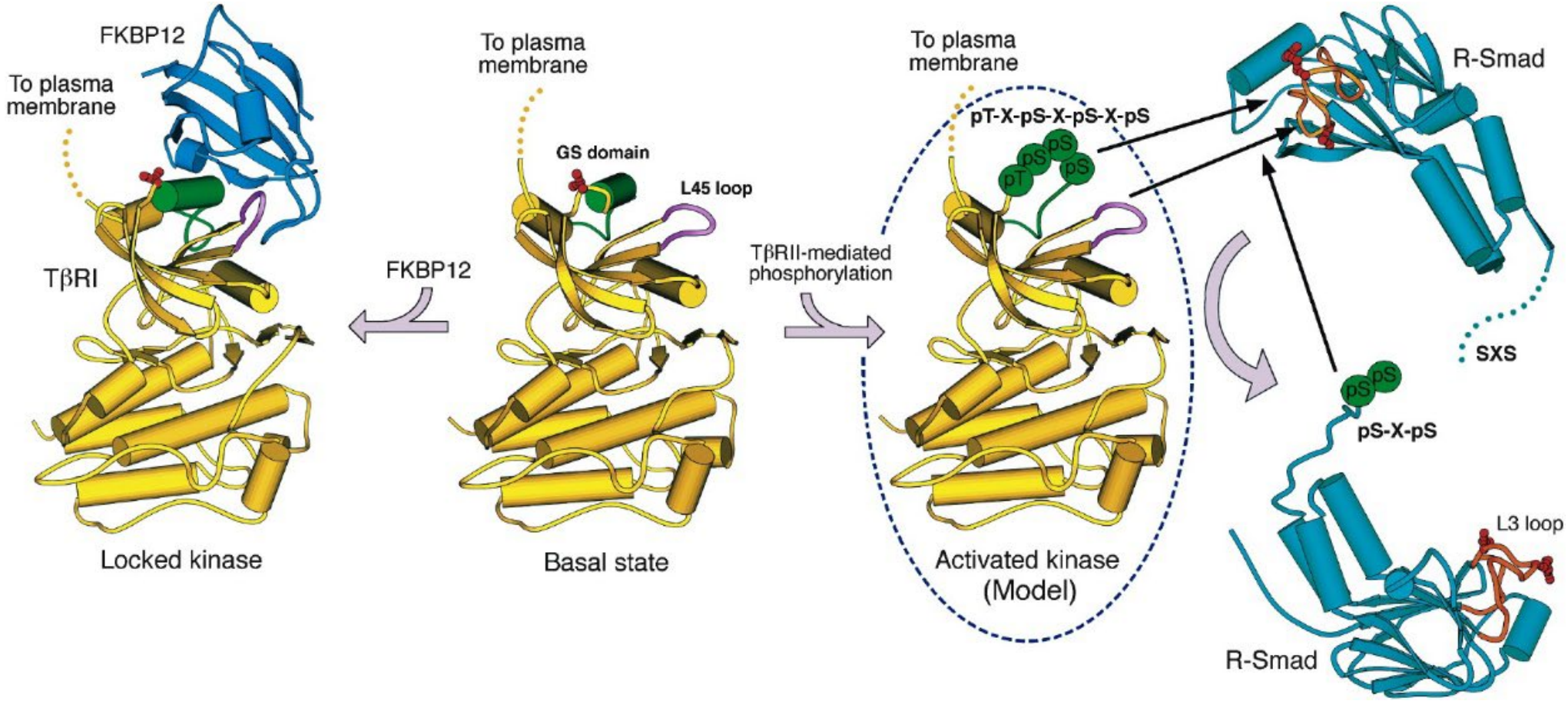

Cell, Vol. 113, 685–700, June 13, 2003

Signaling by TGF-β receptors

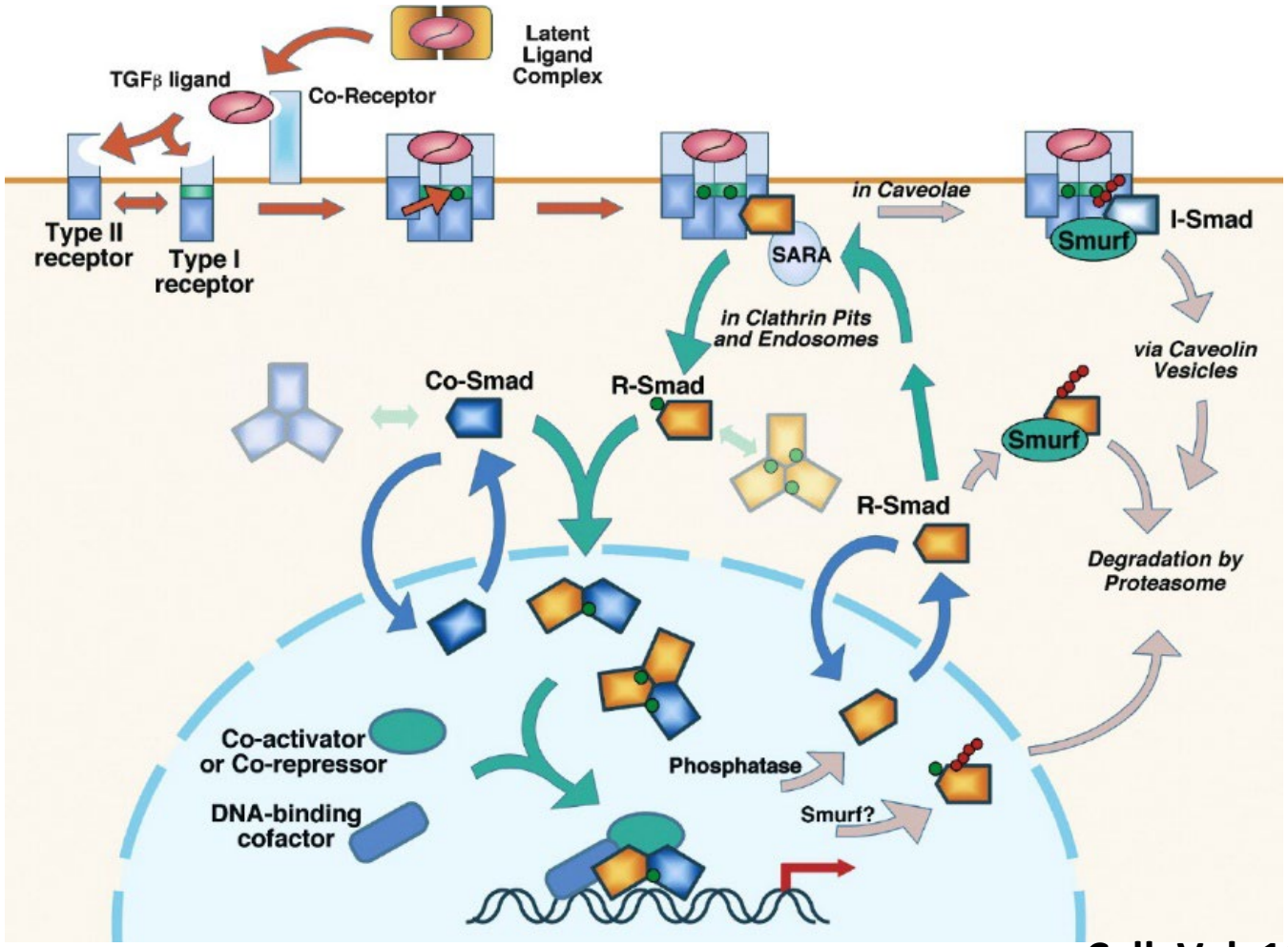

R-smad: 1,2,3,5,8
Co-Smad: 4
I-Smad: 6,7

Cell, Vol. 113, 685–700, June 13, 2003

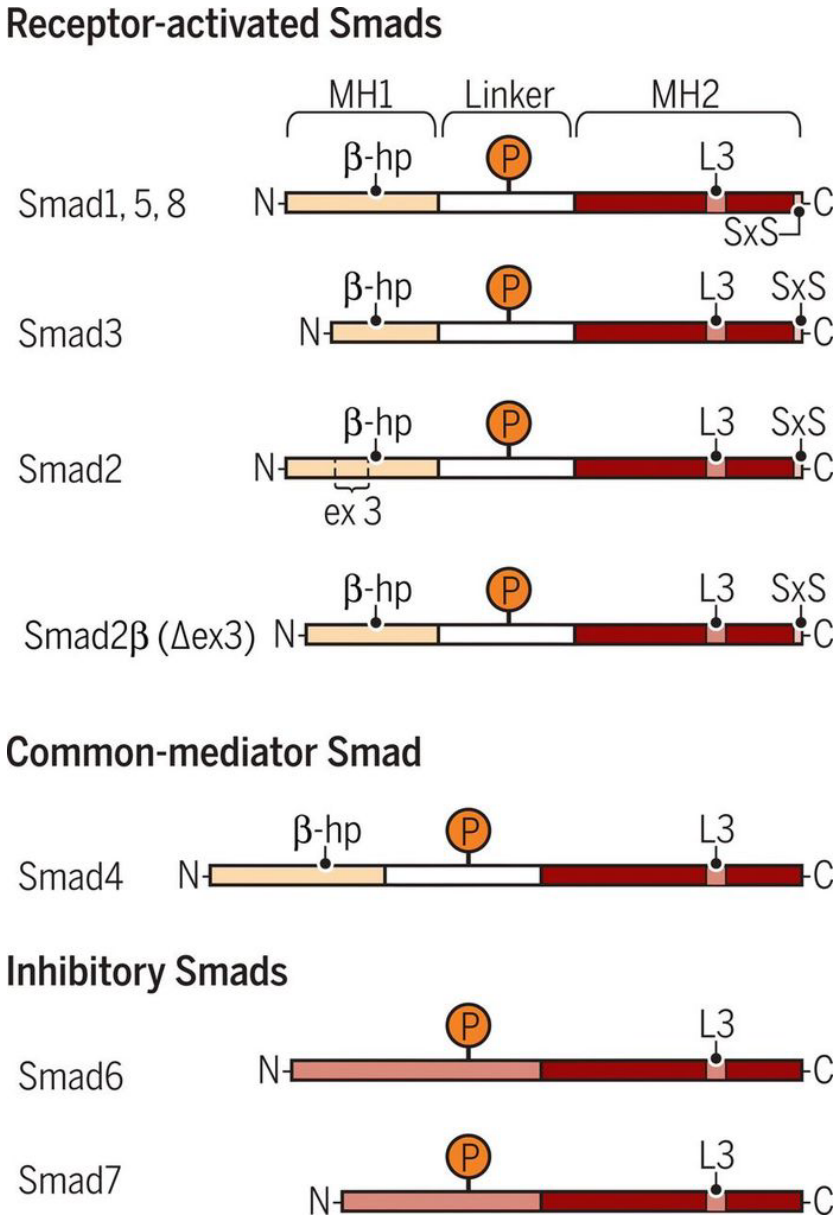

Specificity, versatility, and control of TGF-β family signaling, Volume: 12, Issue: 570, DOI: (10.1126/scisignal.aav5183)

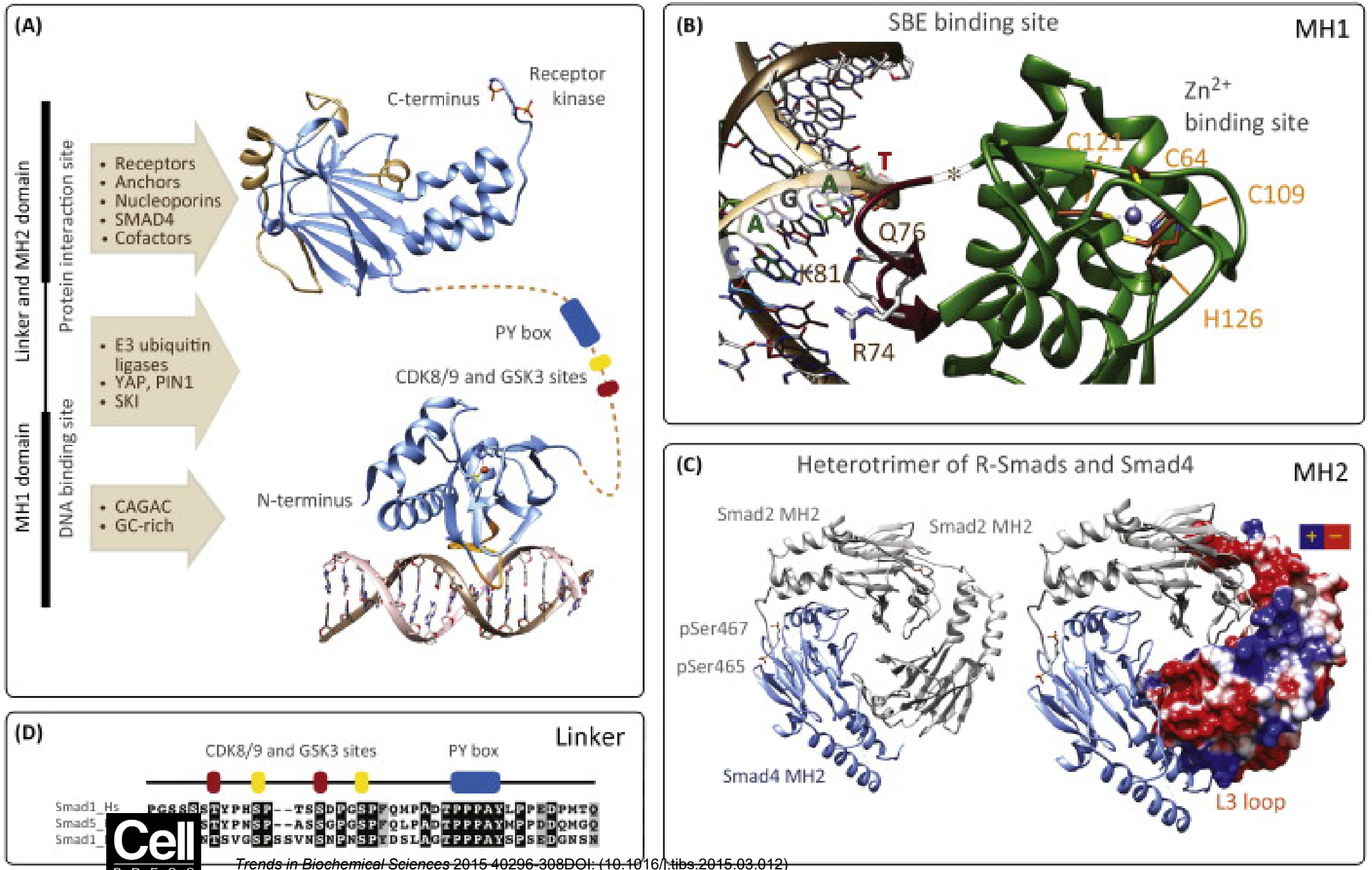

Trends in Biochemical Sciences 2015 40296-308DOI: (10.1016/j.tibs.2015.03.012)

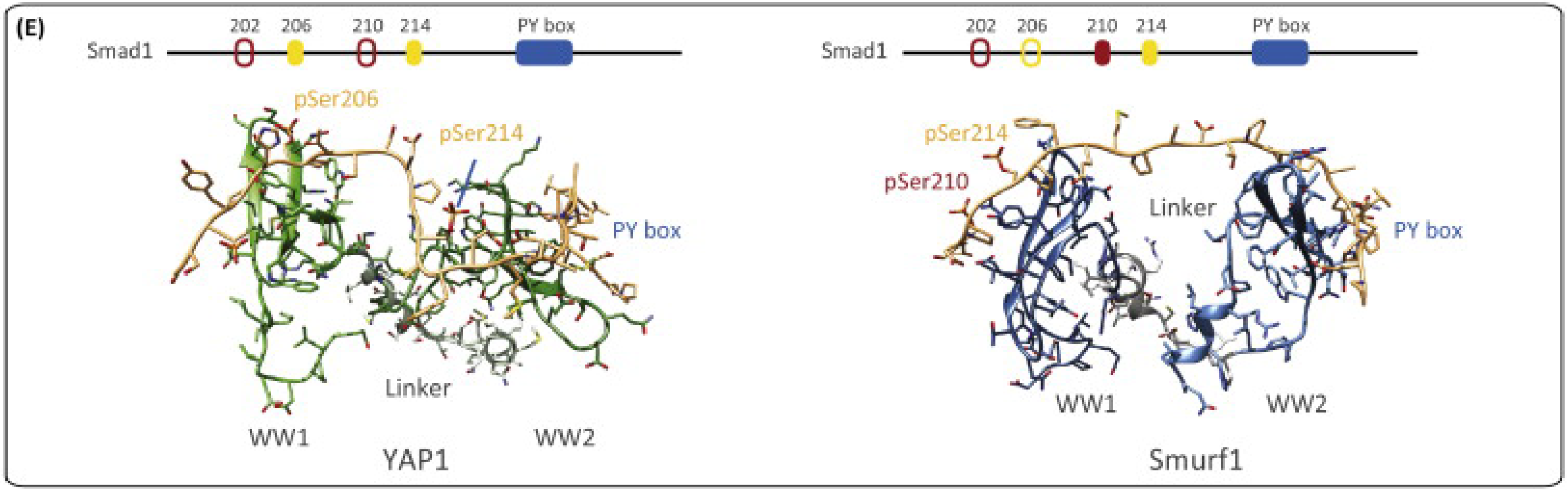

TiBS

Trends in Biochemical Sciences 2015 40296-308DOI: (10.1016/j.tibs.2015.03.012)

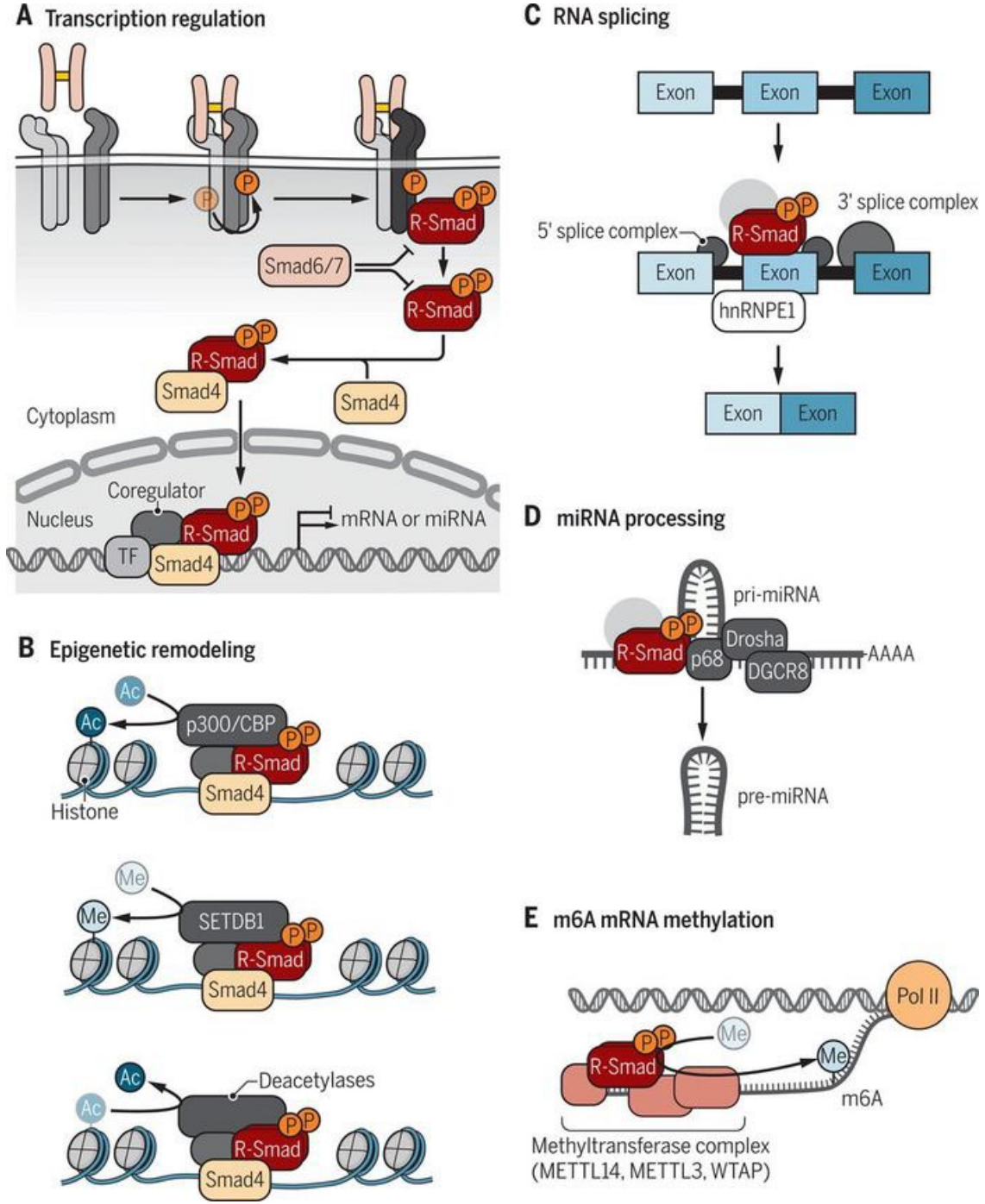

Specificity, versatility, and control of TGF-β family signaling, Volume: 12, Issue: 570, DOI: (10.1126/scisignal.aav5183)

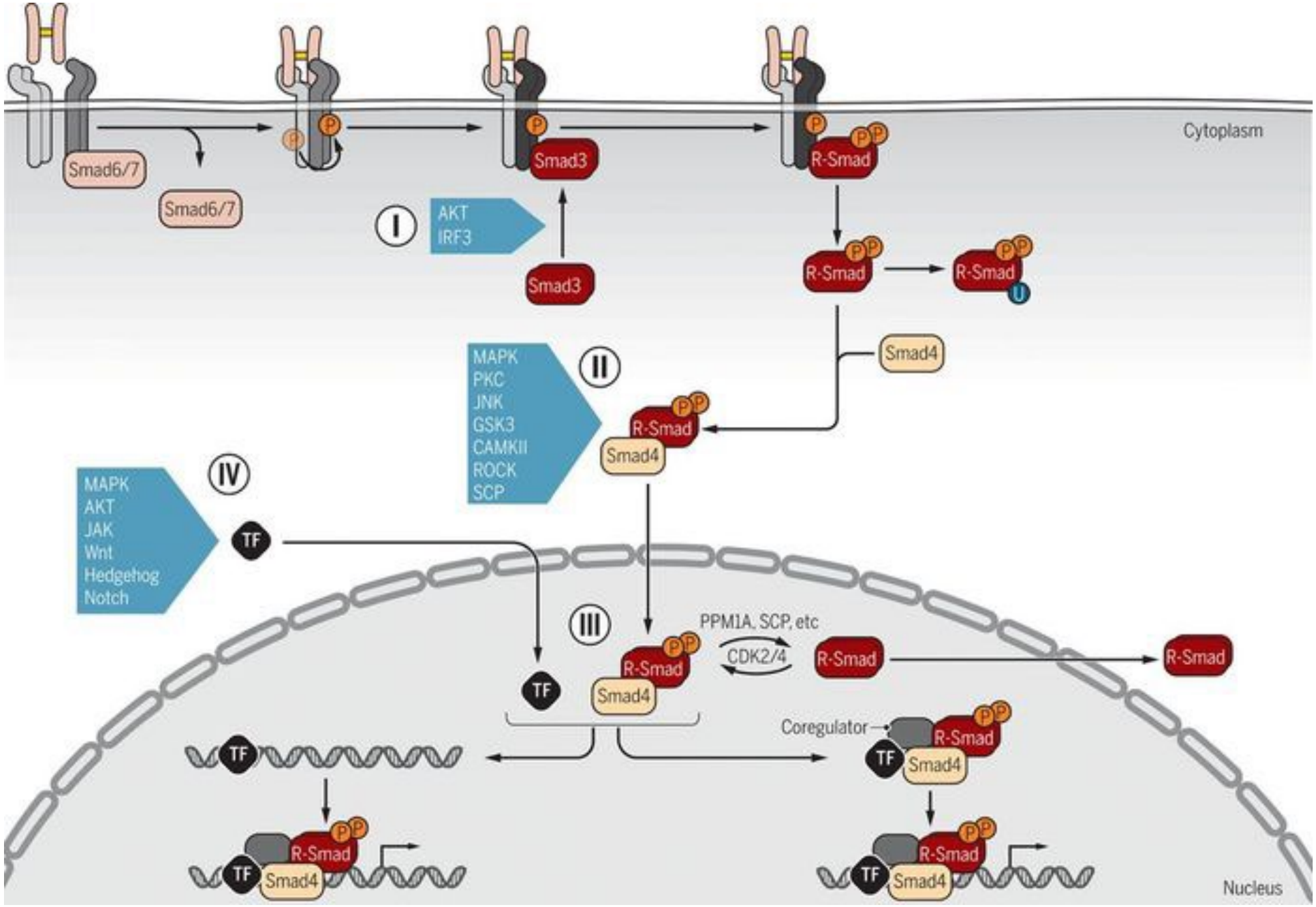

Specificity, versatility, and control of TGF-β family signaling, Volume: 12, Issue: 570, DOI: (10.1126/scisignal.aav5183)

Context-dependent transcription by Smads

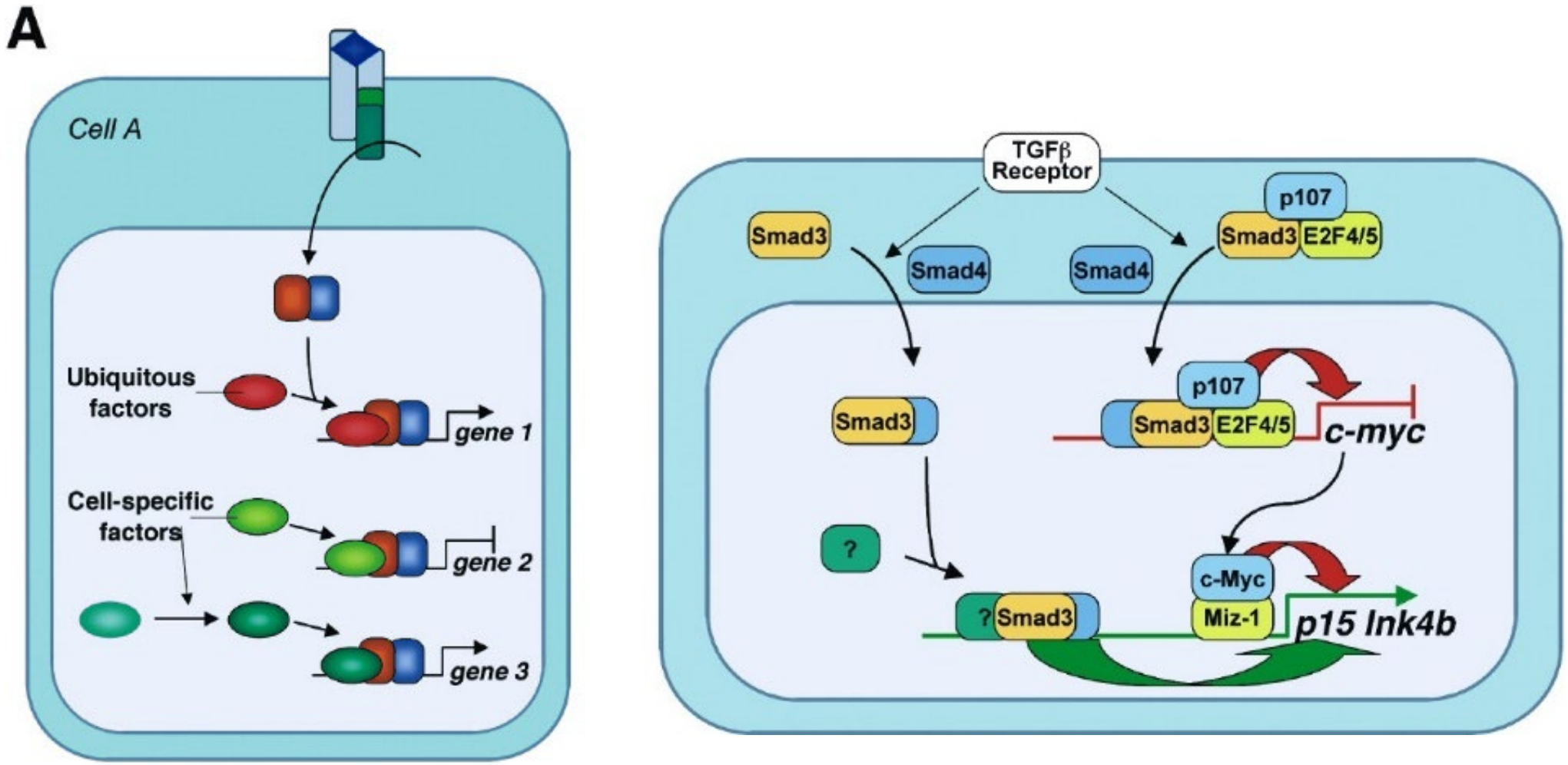

Cell, Vol. 113, 685–700, June 13, 2003

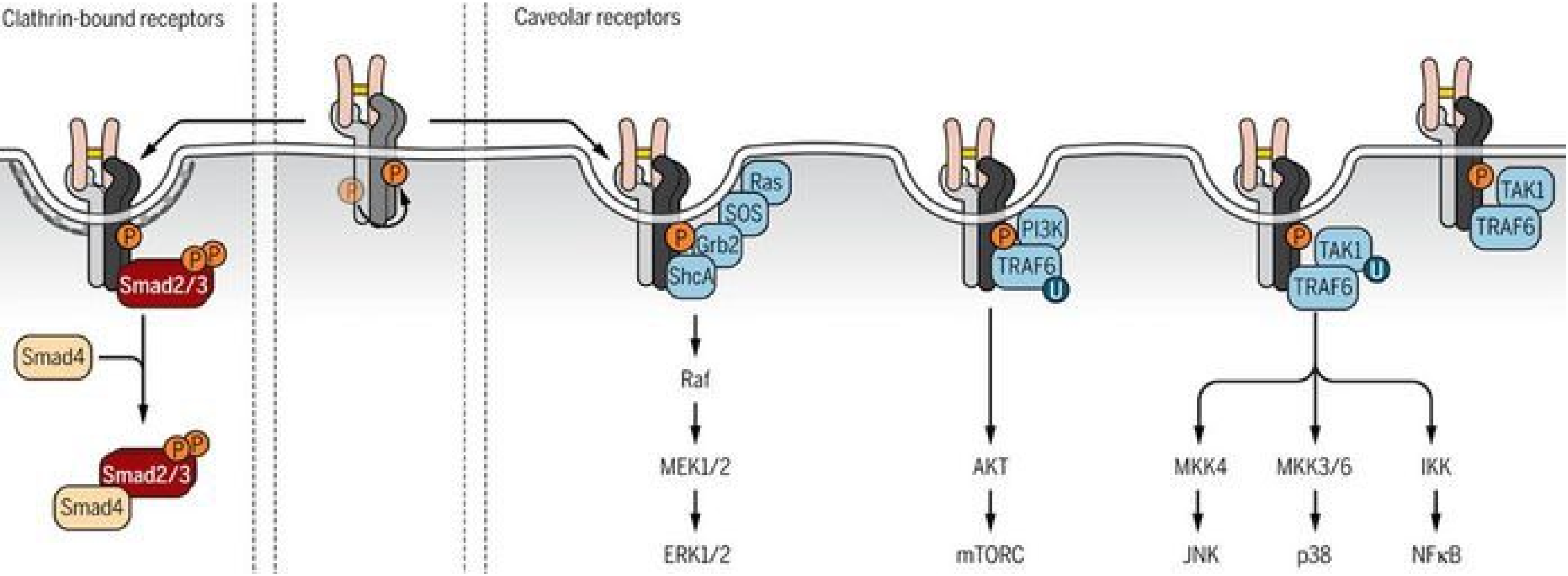

Specificity, versatility, and control of TGF-β family signaling, Volume: 12, Issue: 570, DOI: (10.1126/scisignal.aav5183)

The context-dependent, combinatorial logic of BMP signaling

Heidi E. Klumpe, Matthew A. Langley, James M. Linton, Christina J. Su, Yaron E. Antebi, Michael B. Elowitz
Cell Systems
Volume 13 Issue 5 Pages 388-407.e10 (May 2022)
DOI: 10.1016/j.cels.2022.03.002

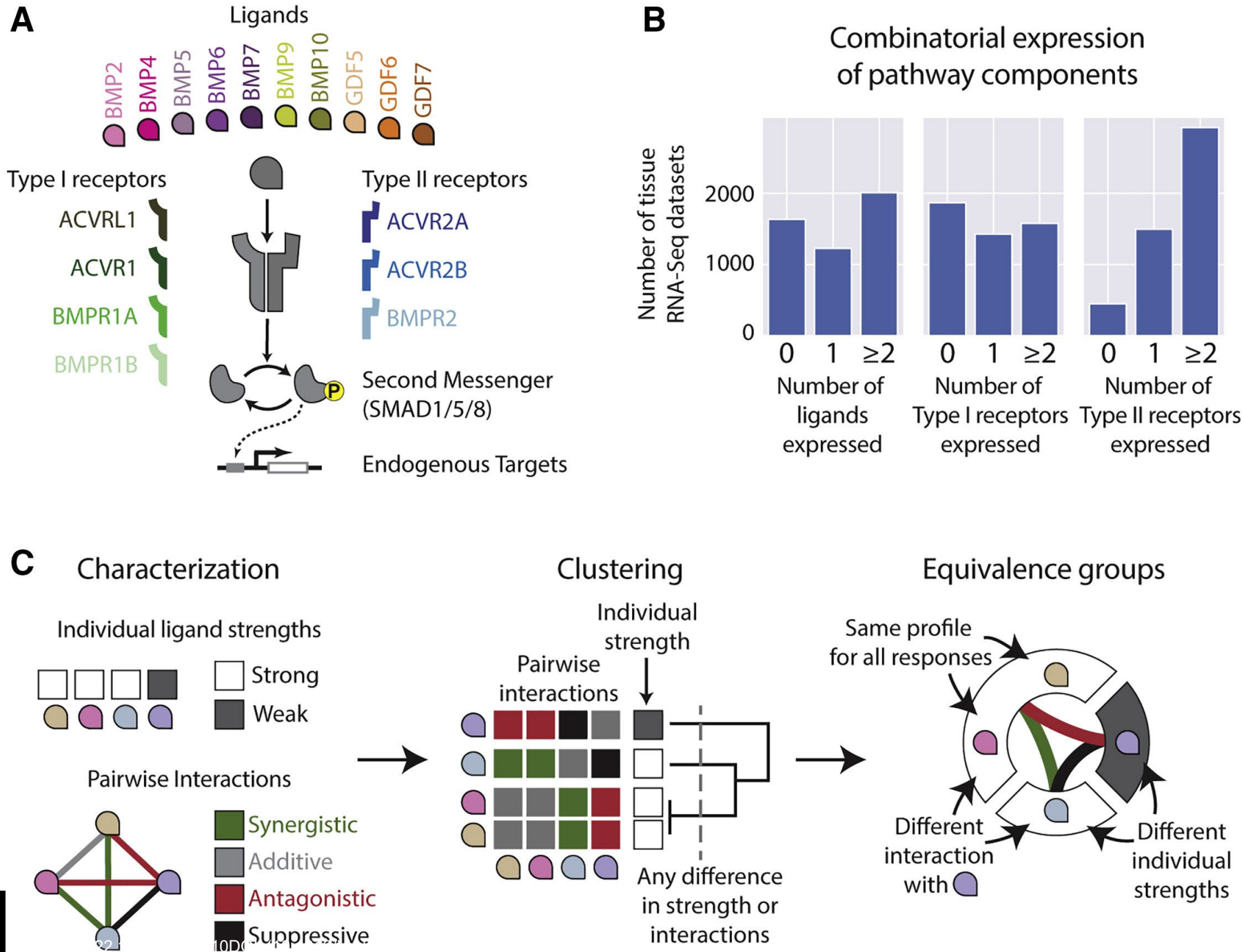

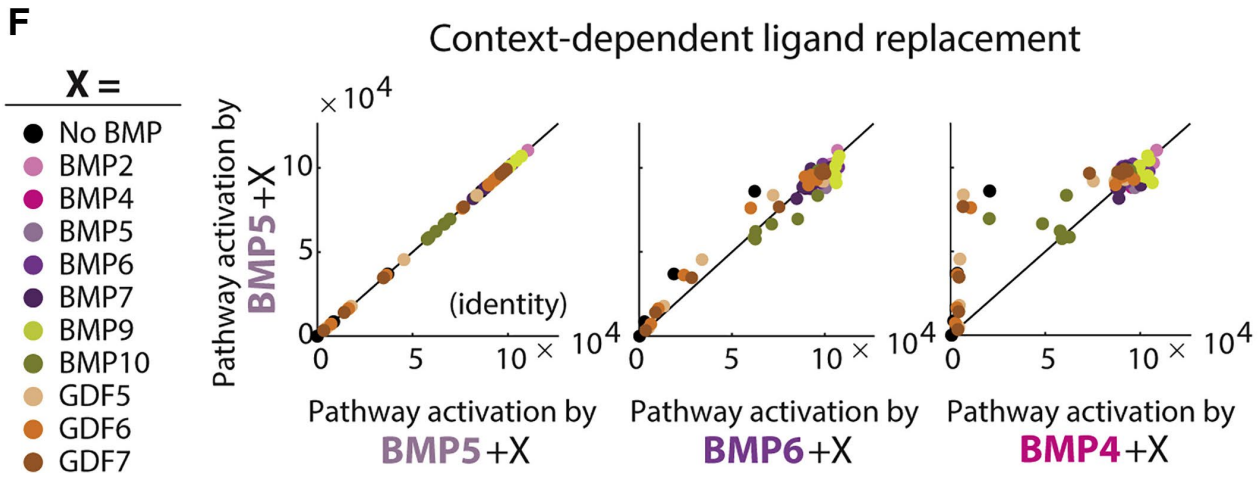

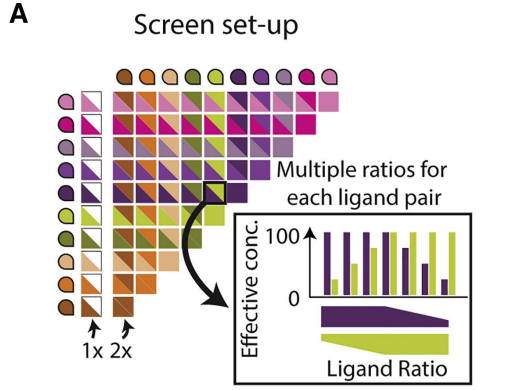

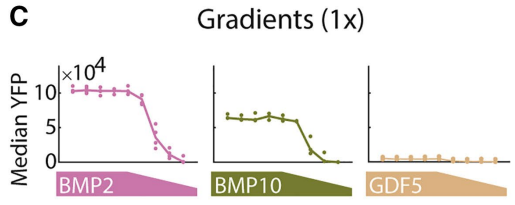

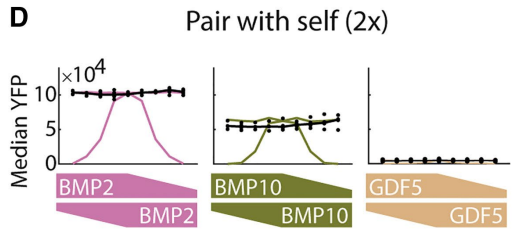

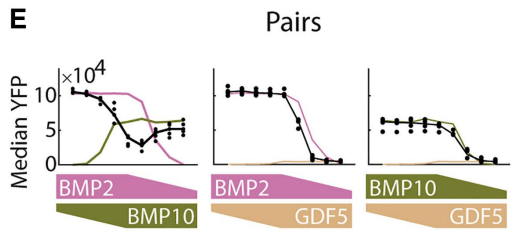

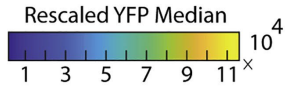

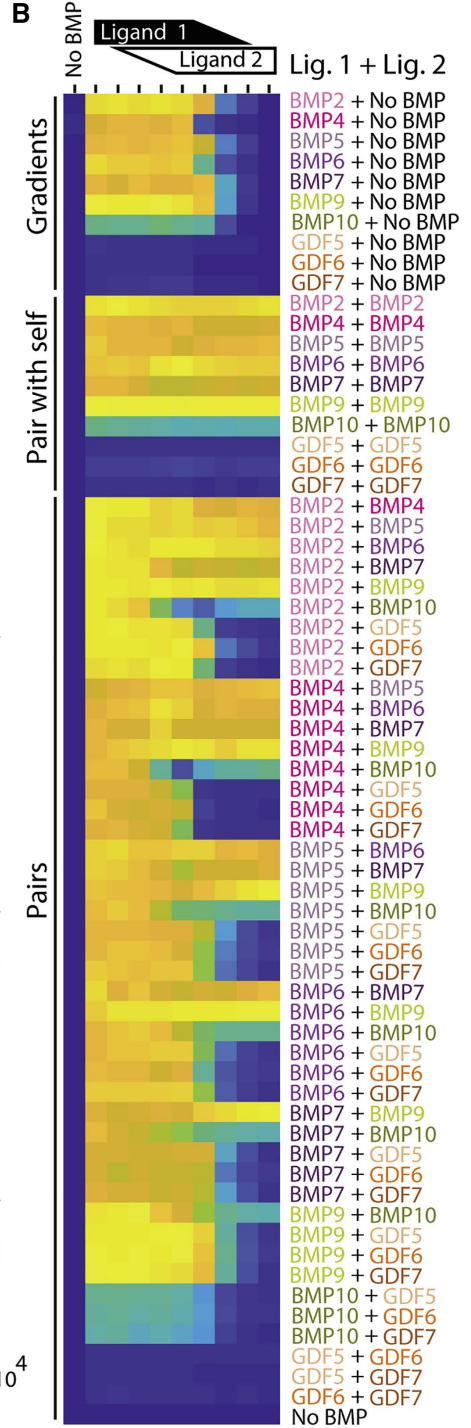

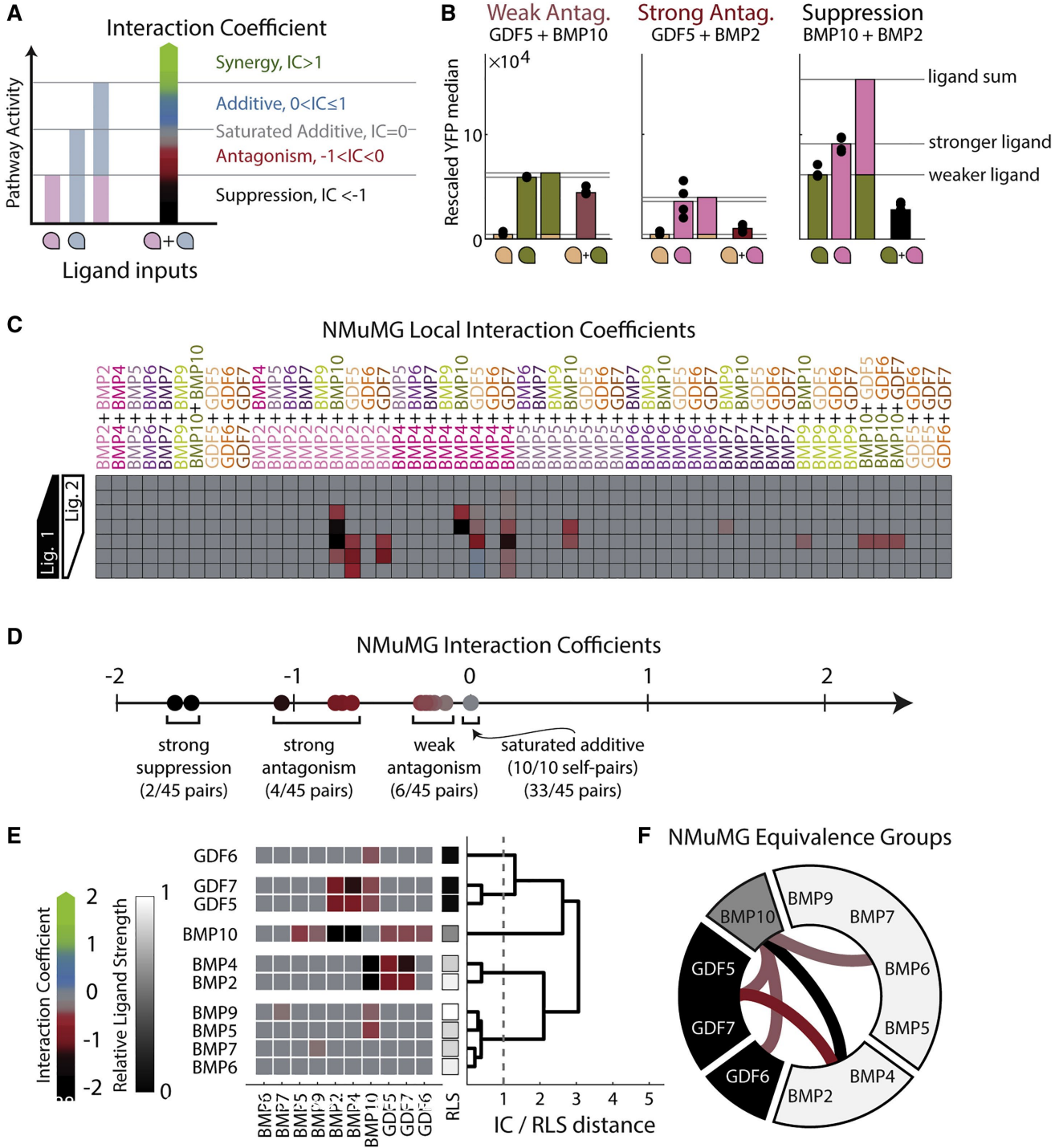
A
Interaction Coefficient
Synergy, IC>1
Additive, 0<IC≤1
Saturated Additive, IC=0
Antagonism, -1<IC<0
Suppression, IC <-1
Pathway Activity
Ligand inputs
B
Weak Antag.
GDF5 + BMP10
Strong Antag.
GDF5 + BMP2
Suppression
BMP10 + BMP2
Rescaled YFP median
×10^4
ligand sum
stronger ligand
weaker ligand
C
NMuMG Local Interaction Coefficients
Lig. 1
Lig. 2
D
NMuMG Interaction Cofficients
strong suppression (2/45 pairs)
strong antagonism (4/45 pairs)
weak antagonism (6/45 pairs)
saturated additive (10/10 self-pairs) (33/45 pairs)
E
Interaction Coefficient
Relative Ligand Strength
RLS
IC / RLS distance
F
NMuMG Equivalence Groups

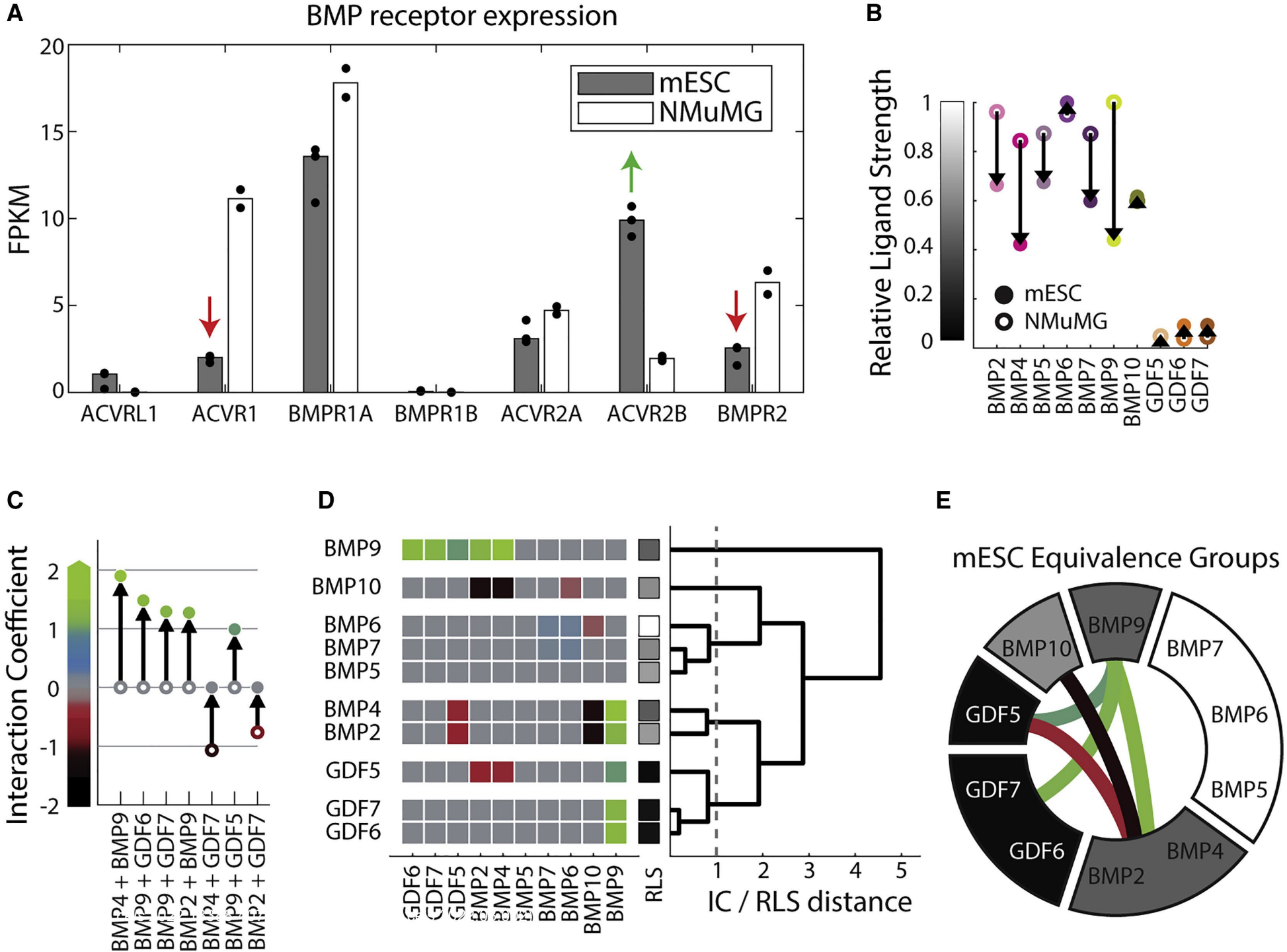
A
BMP receptor expression
FPKM
mESC
NMuMG
ACVRL1
ACVR1
BMPR1A
BMPR1B
ACVR2A
ACVR2B
BMPR2
B
Relative Ligand Strength
mESC
NMuMG
BMP2
BMP4
BMP5
BMP6
BMP7
BMP9
BMP10
GDF5
GDF6
GDF7
C
Interaction Coefficient
BMP4 + BMP9
BMP9 + GDF6
BMP9 + GDF7
BMP2 + BMP9
BMP4 + GDF7
BMP9 + GDF5
BMP2 + GDF7
D
BMP9
BMP10
BMP6
BMP7
BMP5
BMP4
BMP2
GDF5
GDF7
GDF6
RLS
IC / RLS distance
E
mESC Equivalence Groups
BMP9
BMP10
BMP7
BMP6
BMP5
BMP4
BMP2
GDF6
GDF7
GDF5

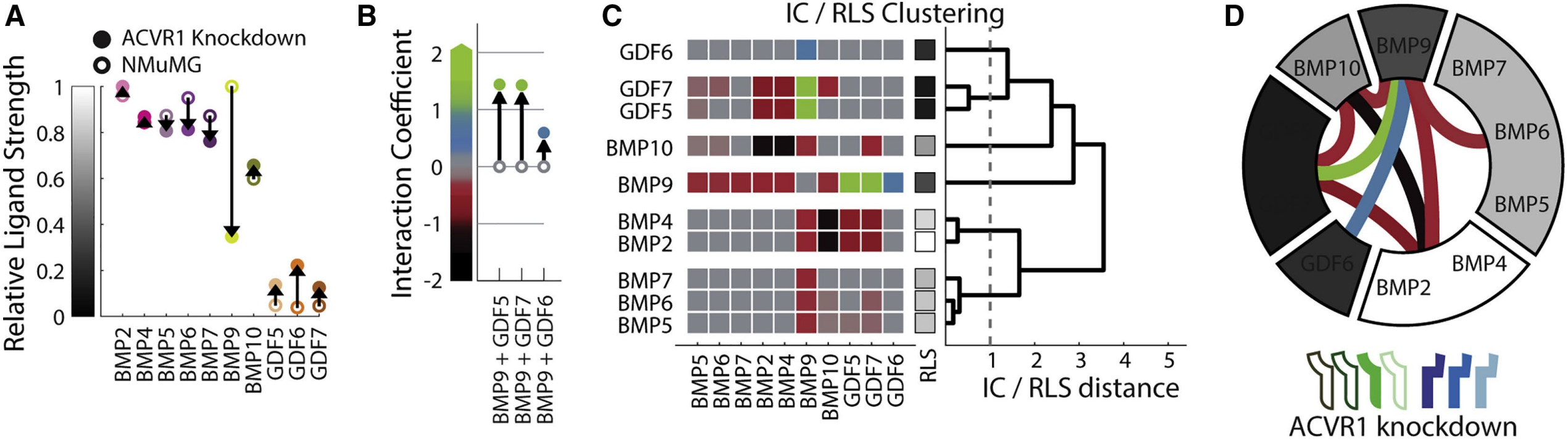

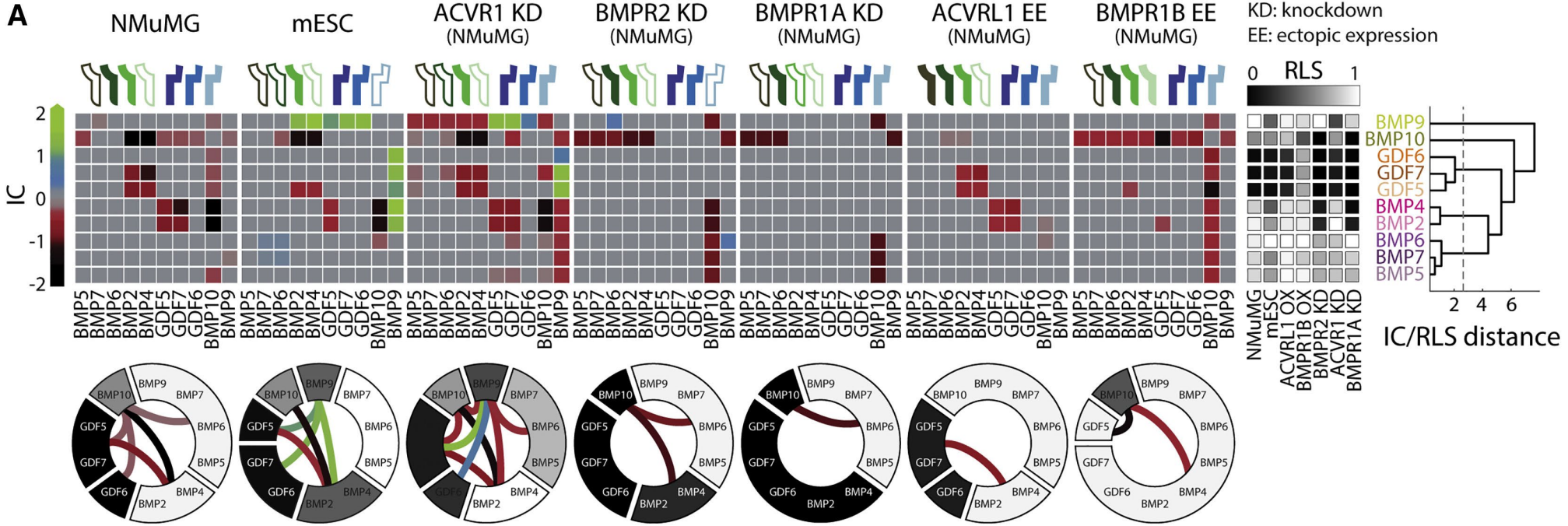

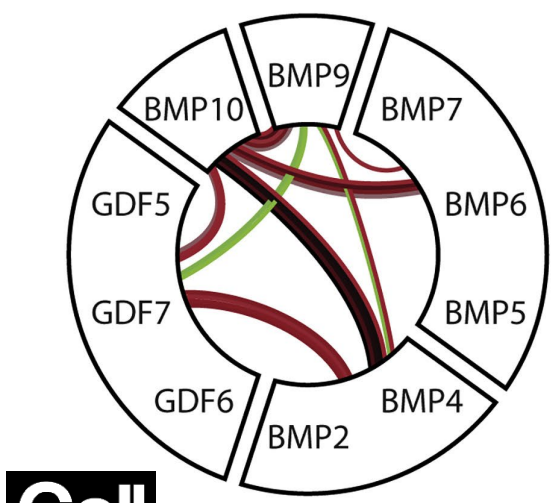

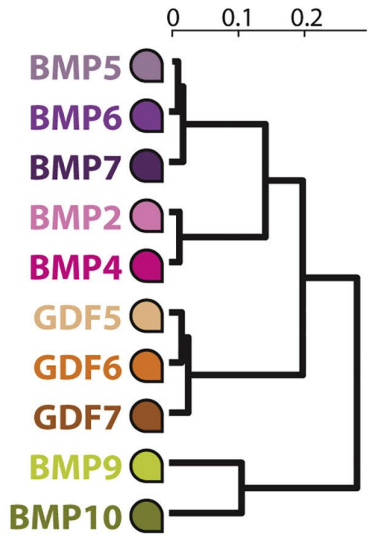

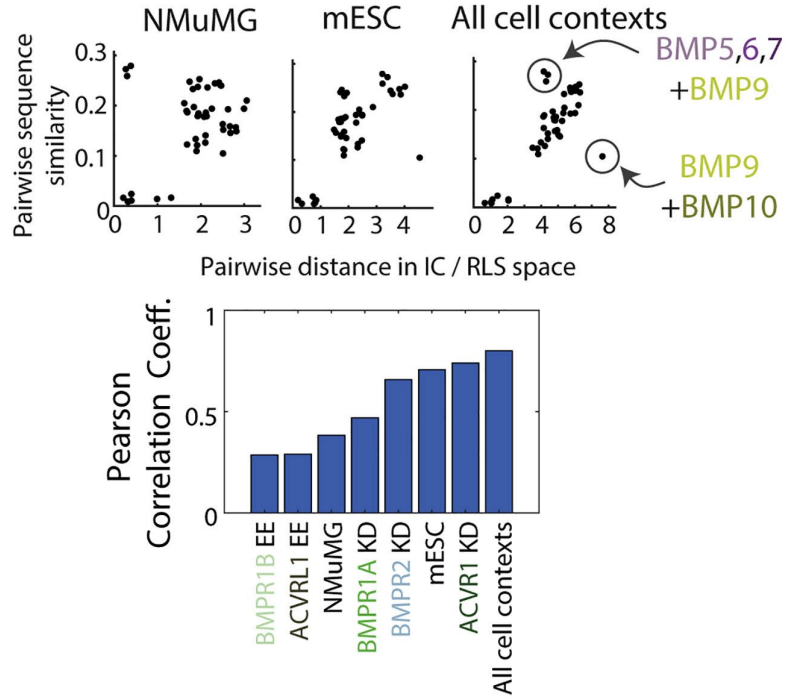

Receptor binding competition as a paradigm for TGF-β family action

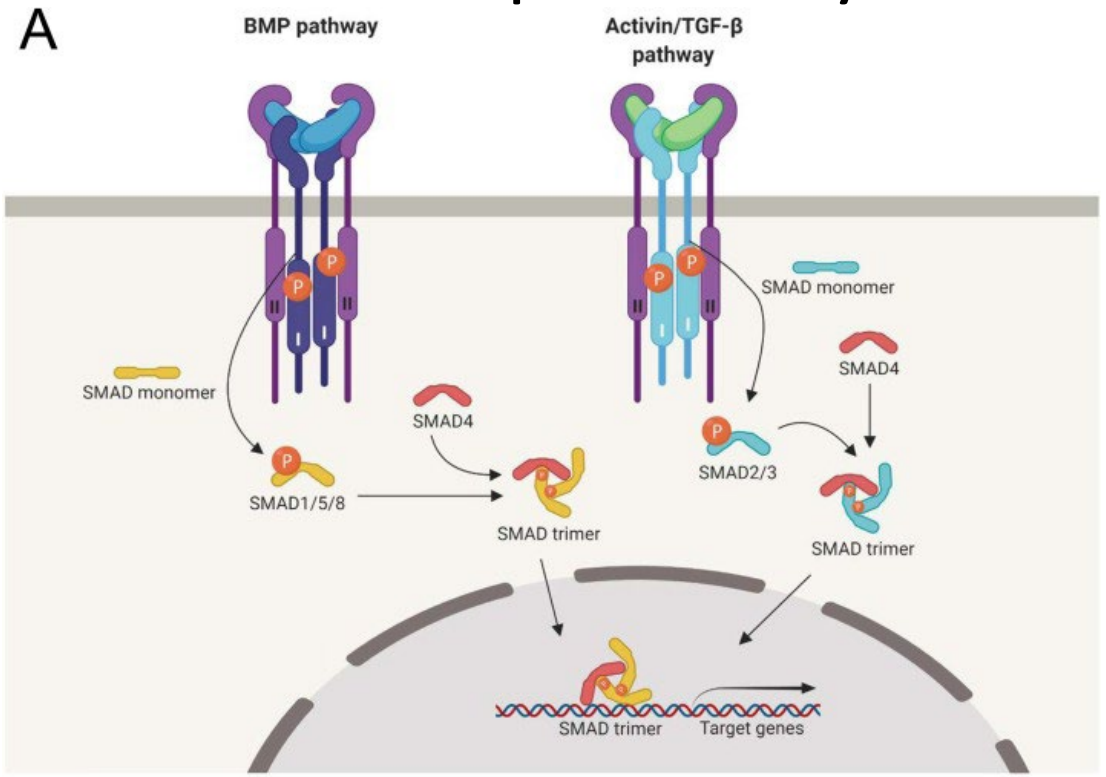

B

Ligands	Type II receptor	Type I receptor	R-SMAD
BMP pathway > 20 ligands	BMPRII (BMPR2) ActRIIA (ACVR2A) ActRIIB (ACVR2B) AMHRII (AMHR2)	ALK1 (ACVRL1) ALK2 (ACVR1) ALK3 (BMPR1A) ALK6 (BMPR1B)	SMAD1 SMAD5 SMAD8
Activin/TGF-β pathway > 15 ligands	ActRIIA (ACVR2A) ActRIIB (ACVR2B) TGFβRII (TGFBR2)	ALK4 (ACVR1B) ALK7 (ACVR1C) ALK5 (TGFBR1)	SMAD2 SMAD3

Cytokine & Growth Factor Reviews Volume 57, February 2021, Pages 39-54

Promiscuous binding by TGF-β ligands

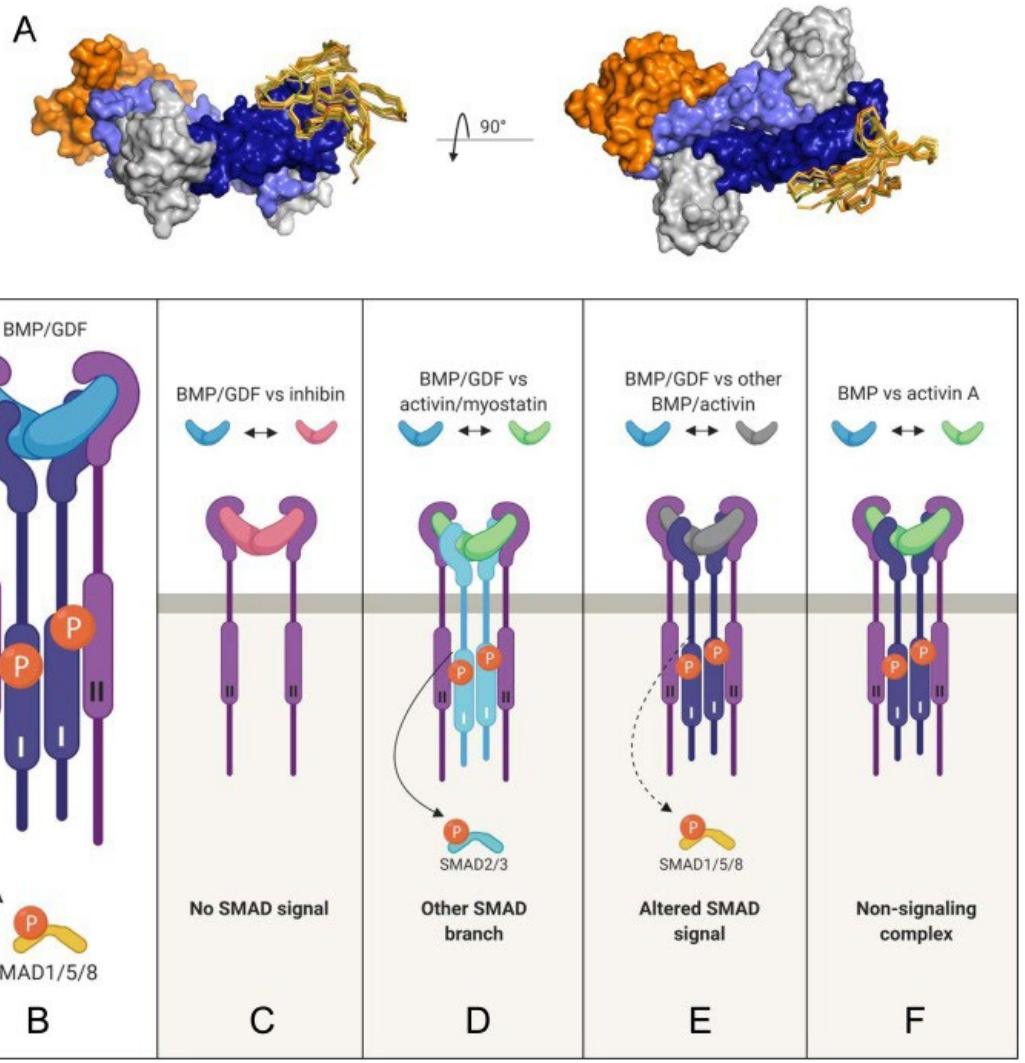

Cytokine & Growth Factor Reviews Volume 57, February 2021, Pages 39-54

Measuring ligand competition

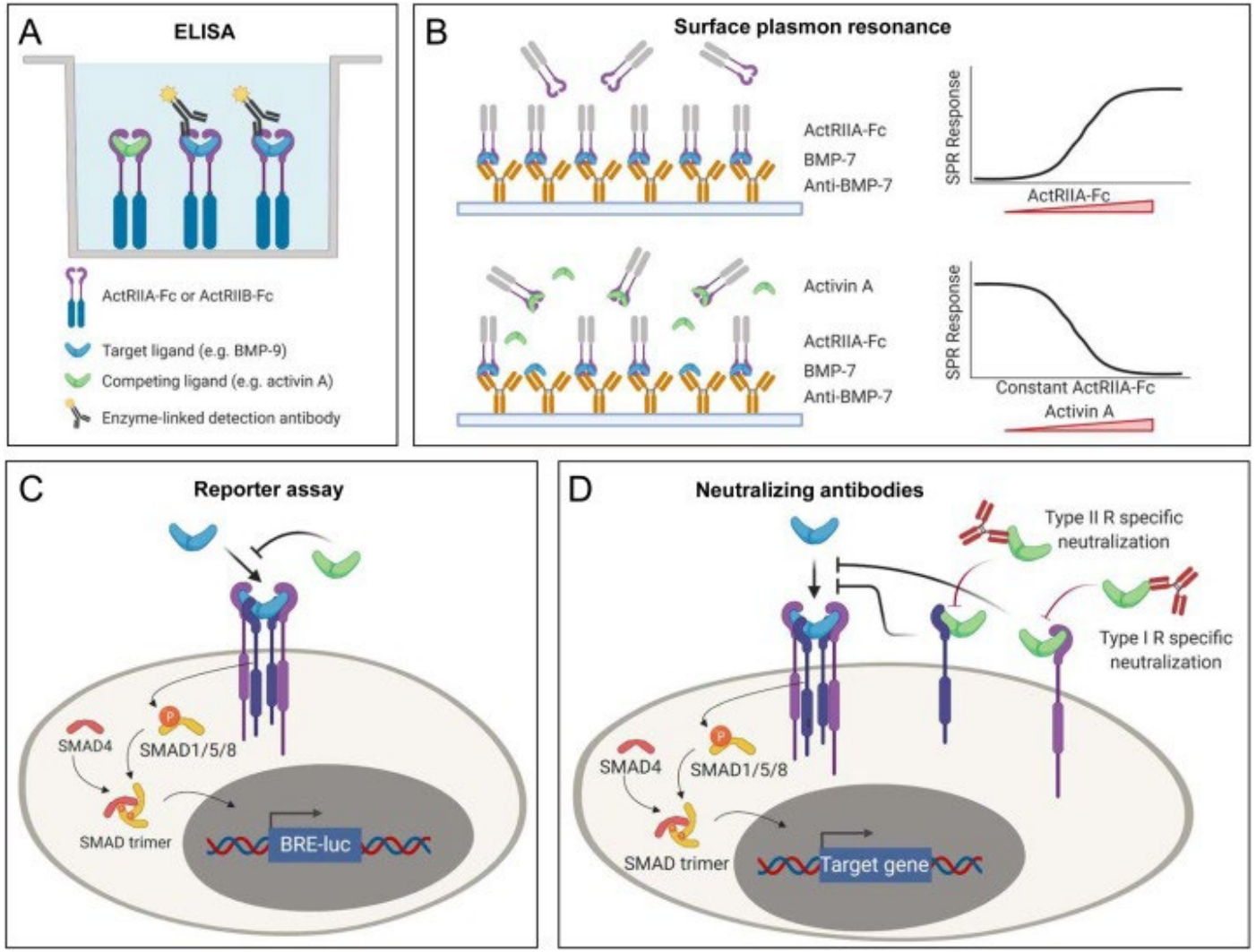

Cytokine & Growth Factor Reviews Volume 57, February 2021, Pages 39-54

Pathological roles of ligand competition

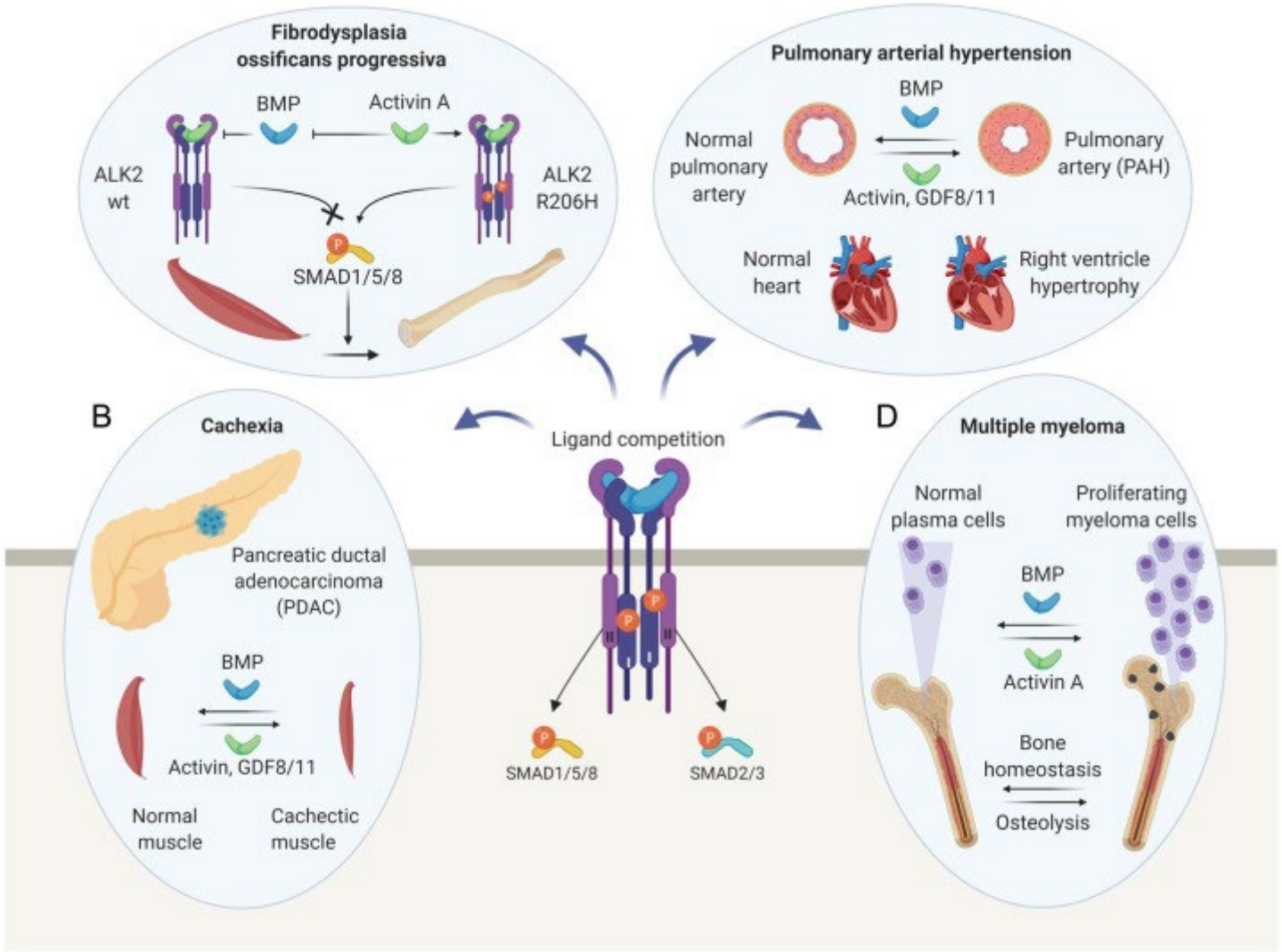

Cytokine & Growth Factor Reviews Volume 57, February 2021, Pages 39-54

Pulmonary Arterial Hypertension

- Disease of the pulmonary vasculature
- Insidious onset - Frequently only symptom is shortness of breath
- Leads to progressive RV dysfunction, failure and ultimately death

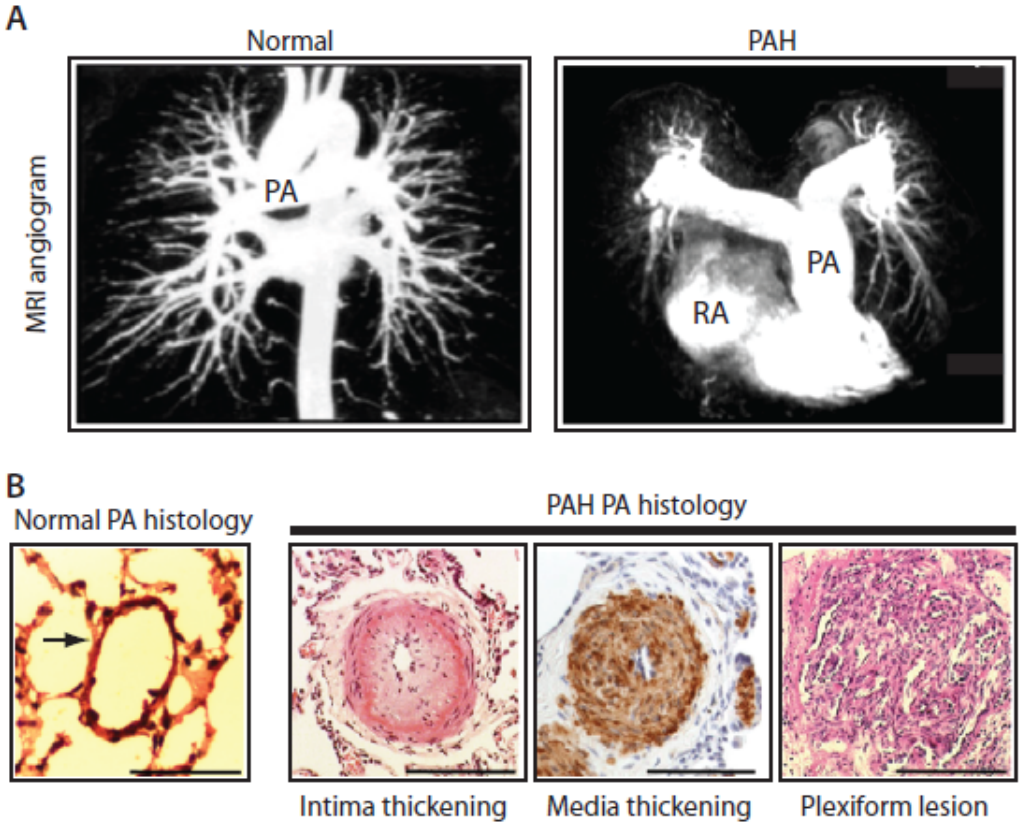

www.ScienceTranslationalMedicine.org 23 October 2013 Vol 5 Issue 208 208sr5

Proposed Mechanism of Action for Sotatercept in Pulmonary Arterial Hypertension.

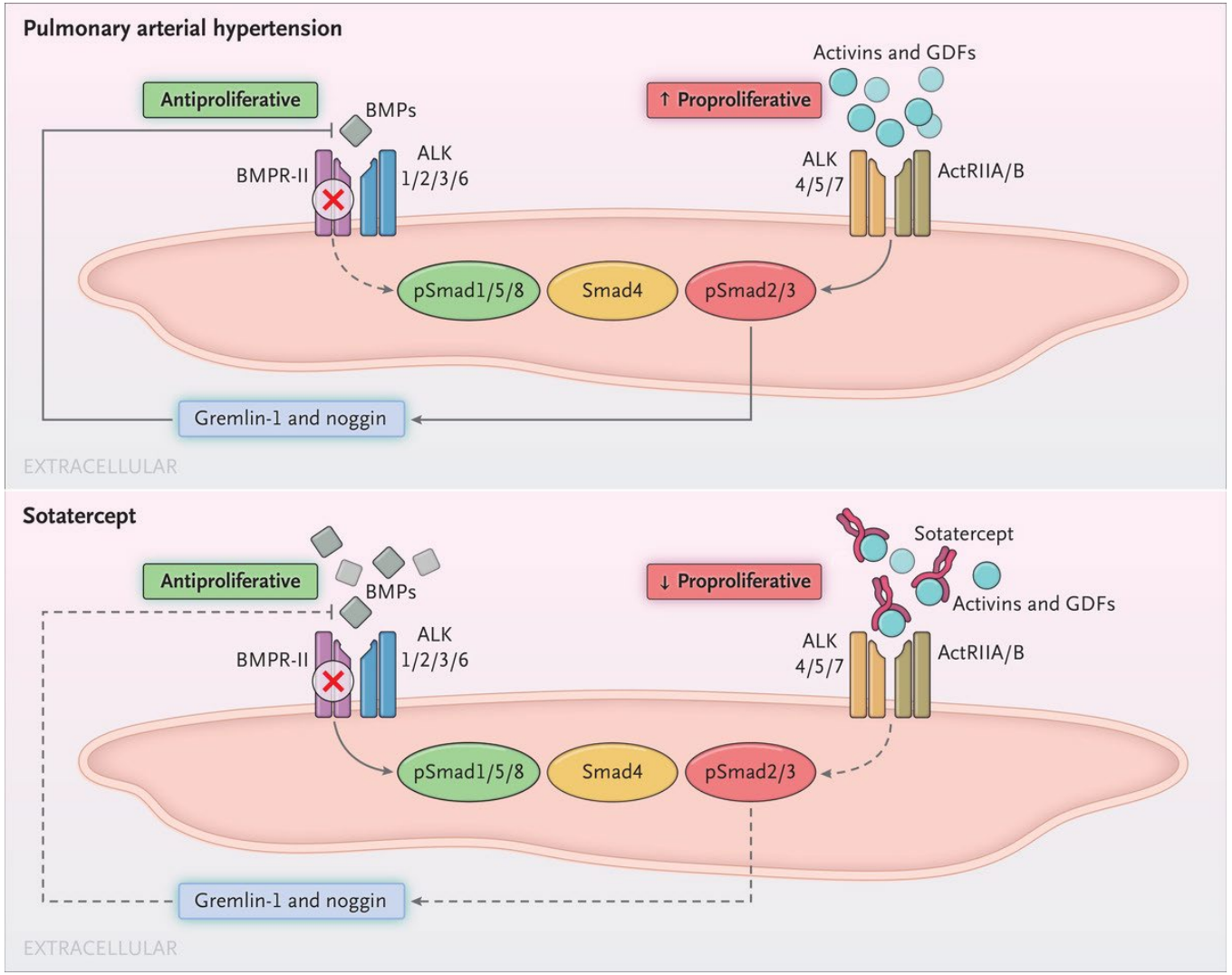

M Humbert et al. N Engl J Med 2021;384:1204-1215.

ACTRIIA-Fc modulates signaling, gene regulation, and proliferation of human pulmonary vascular cells.

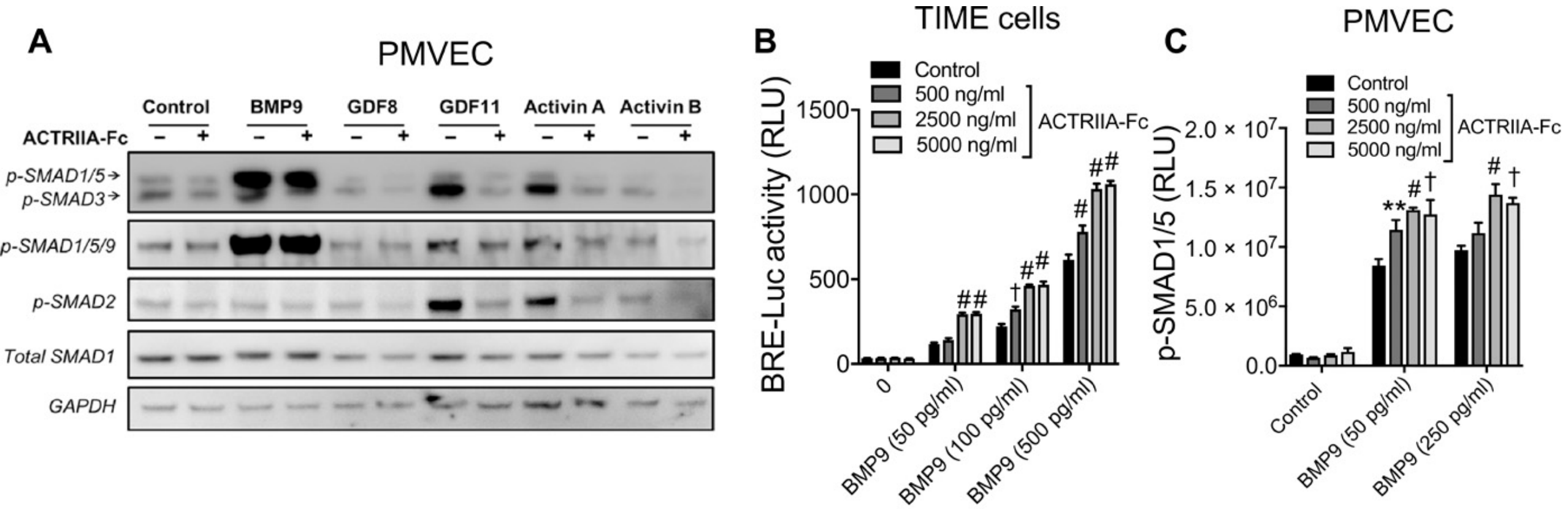

Lai-Ming Yung et al., Sci Transl Med 2020;12:eaaz5660

Science Translational Medicine
AAAS

Change in Pulmonary Vascular Resistance from Baseline to Week 24 in the Intention-to-Treat Population.

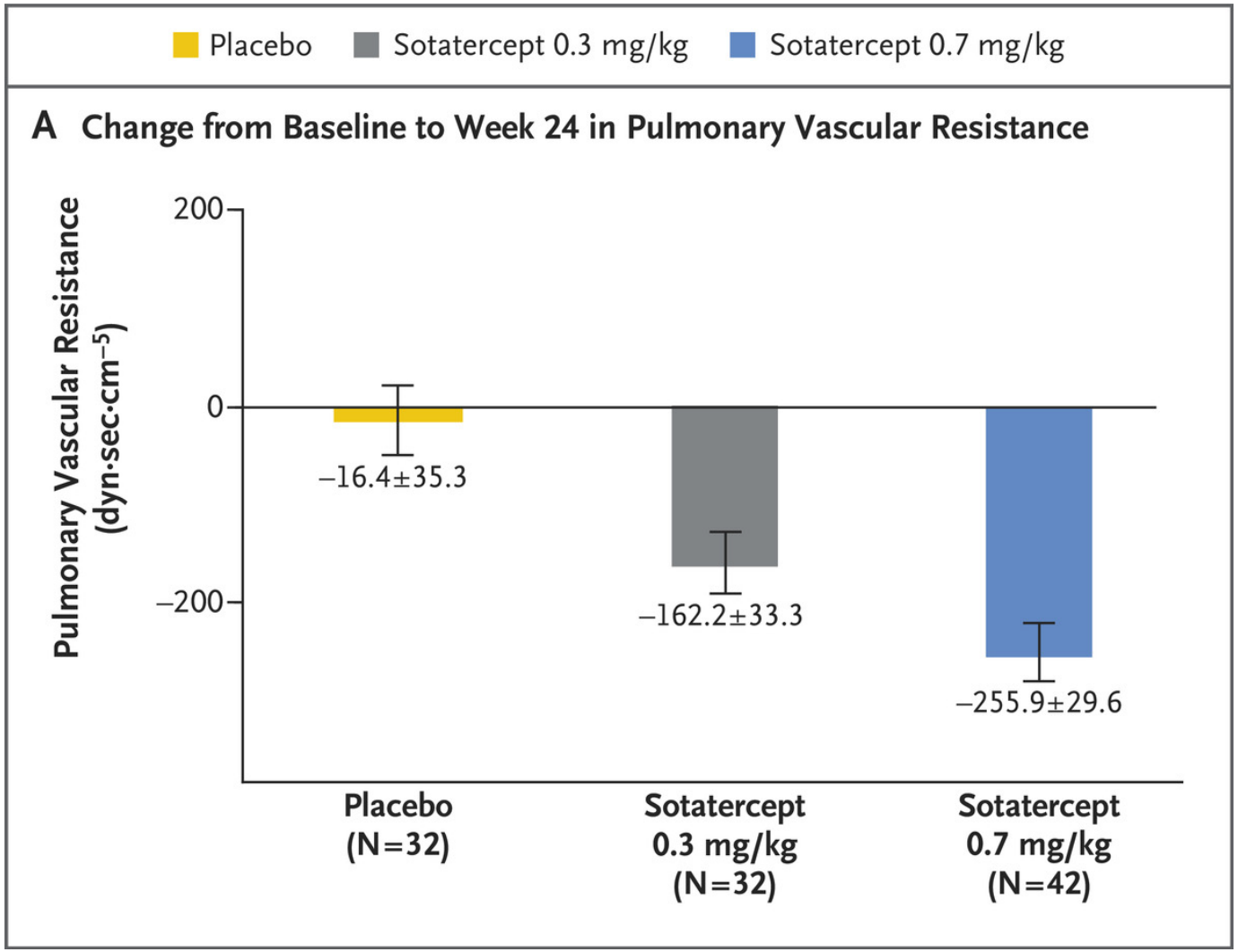

M Humbert et al. N Engl J Med 2021;384:1204-1215.